Garnet-quartz intergrowths in granitic pegmatites from Bergell and Adamello, Italy

by *Chunfu Zhang[1], Reto Gieré[1], Holger Stünitz[2], Peter Brack[3] and Peter Ulmer[3]*

Abstract

Garnet-quartz intergrowths characterized by graphic texture have been found in granitic pegmatites at three localities in Italy (Sivigia and Val Bona, Bergell; Val Caffaro, Adamello). The intergrowths form nodules which are up to several centimeters across and are embedded in a matrix consisting of coarse-grained muscovite, potassium feldspar, plagioclase and quartz. Electron probe microanalysis revealed that garnet is predominantly a spessartine-almandine solid solution with spessartine contents as high as 78 mol%. Within the intergrowths, individual garnet lamellae are often zoned, whereby the spessartine content decreases considerably from the center to the rim. Some lamellae, however, display only weak zoning or are chemically homogeneous.

X-ray texture goniometry data suggest that the examined area within a nodule at Sivigia consists of a single garnet crystal which is intergrown with a single quartz crystal, whose c-axis is oriented between the poles to (011) and (112) of garnet. At Adamello, the garnet consists of a single crystal, but the intergrown quartz is a polycrystalline aggregate.

Oxygen isotope data for mineral separates from the Sivigia pegmatite revealed that the $\delta^{18}O_{SMOW}$ values for quartz within the intergrowths are identical to those of quartz occurring in the pegmatite matrix (11.8‰). Oxygen isotope thermometry indicates an equilibration temperature of approximately 720 °C for coexisting garnet and quartz. The high $\delta^{18}O$ values of all major minerals suggest that the Sivigia pegmatite melt may have been derived from metasedimentary rocks, in agreement with whole-rock geochemical data. Moreover, the normal sequence of $\delta^{18}O$ values exhibited by the major minerals indicates that the pegmatite was not subjected to significant postmagmatic hydrothermal alteration. The observations are consistent with a magmatic origin of the garnet-quartz intergrowths. The intergrowth texture indicates that garnet and quartz crystallized simultaneously from the granitic melt, probably as a result of cotectic crystallization.

Keywords: garnet, quartz, intergrowth, pegmatite, Bergell, Adamello.

1. Introduction

Intergrowths of garnet and quartz in granitic pegmatites are an intriguing petrographic and textural feature, with an appearance similar to graphic intergrowths of quartz and alkali feldspar. Such intergrowths have only rarely been reported, for example from the Gaya District, India (ROY, 1935); Adamello, Italy (ULMER, 1982); Bergell, Italy (GIERÉ, 1984; GIERÉ, 1987); East Antarctica (SUZUKI and MATSUMOTO, 1989); the Belomorian province, Russia (SOKOLOV and KHLESTOV, 1990); and Oberpfalz, Germany (LINHARDT, 2000). Garnet-quartz intergrowths are more common than one might suspect on the basis of the few reported occurrences; they have been observed at several other localities including: Wolf Mountain Intrusion in Texas, USA (R. Reed, personal communication, 1999); Left Hand Canyon, Boulder County, Colorado, USA (R.J. Swope, personal communication, 2000); Ticino, Switzerland; and Olgiasca, Lago di Como, Italy. Samples from Ticino and Olgiasca are on display at the Mineralogical Museum at ETH Zürich, and another sample from Bergell is on display in the Bergell Valley Museum, Ciäsa Granda in Stampa, Switzerland.

[1] Department of Earth and Atmospheric Sciences, Purdue University, West Lafayette, IN 47907-1397, USA.
   <giere@purdue.edu>
[2] Geologisches Institut der Universität Basel, Bernoullistrasse 32, CH-4056 Basel, Switzerland.
[3] Institut für Mineralogie und Petrographie, ETH Zentrum, CH-8092 Zürich, Switzerland.

Garnet is a common accessory mineral in per-aluminous granitic rocks, where it is usually subhedral to euhedral (HALL, 1965; SATHE, 1968; CLARKE, 1981; KISTLER et al., 1981; MANNING, 1983; HARRISON, 1988; SOKOLOV and KHLESTOV, 1990; PUZIEWICZ, 1990; MacLeod, 1992; WHITWORTH, 1992; BOGOCH et al., 1997). It is most commonly a spessartine-almandine solid solution (CALLEGARI, 1966; JAFFE, 1951; MILLER and STODDARD, 1981; STONE, 1988; YERMOLOV et al., 1979). It may contain a significant amount of Yttrium (HARRISON, 1988; JAFFE, 1951; KASOWSKI and HOGARTH, 1968), and in one case, a grossular-dominant composition has been reported (SATHE, 1968). Even though garnet in granitic rocks is often chemically homogeneous, there are many examples of various types of compositional zoning (BALDWIN and VON KNORRING, 1983; FOORD, 1976). Garnet frequently exhibits normal zoning (CLARKE, 1981), i.e., the Fe content increases from core to rim, with a concomitant decrease in Mn (BOGOCH et al., 1997; LEAKE, 1967; MACLEOD, 1992; MANNING, 1983; MILLER and STODDARD, 1981). However, garnet may also display reverse zoning (CLARKE, 1981), i.e., the Fe content decreases towards the rim (MANNING, 1983; PUZIEWICZ, 1990). In some cases, more complex zoning patterns can be observed (GIERÉ, 1984). PUZIEWICZ (1990) summarized three major factors leading to an accumulation of Mn in granitic garnets: decreasing pressure (see also GREEN, 1977), increasing Mn concentration due to the crystallization of Mn-incompatible minerals in a magma (MILLER and STODDARD, 1981), and increasing oxygen fugacity (HSU, 1968).

The origin of garnets in granitic rocks has been attributed to various processes: (1) primary magmatic crystallization (ABBOTT, 1981; DU BRAY, 1988; HALL, 1965; HARRISON, 1988; HENTSCHKE, 1987; JOYCE, 1973; MILLER and STODDARD, 1981; STONE, 1988); (2) reaction between silicate melt and such phases as biotite and cordierite, which crystallized earlier (ABBOTT and CLARKE, 1979; MILLER and STODDARD, 1978, 1981); (3) reaction between melt and Al- and Mn-rich pelitic xenoliths (ALLAN and CLARKE, 1981; JAMIESON, 1974); (4) derivation from allochthonous sources, e.g., garnet as a refractory phase from the partial melting zone in migmatite terrains (BELLIENI et al., 1979; CHAPPELL and WHITE, 1974; GREEN, 1977; STONE, 1988; WHITE and CHAPPELL, 1977) or as a xenocryst from the country rocks (ABBOTT, 1981; ALLAN and CLARKE, 1981; BIRCH and GLEADOW, 1974; VENNUM and MEYER, 1979; WHITWORTH, 1992; ZECK, 1970); (5) metamorphic growth in syntectonic granitoids (WEIGAND et al., 1981); and (6) post-

magmatic hydrothermal crystallization (PUZIEWICZ, 1990).

Graphic texture, often observed in granites and pegmatites (LONDON, 1996), refers to an intergrowth of quartz and alkali feldspar in which blebs of quartz lie in crystallographically controlled orientations within large alkali feldspar crystals (SMITH, 1974). Similar textures involving other pairs of minerals are also known, but are often less regular. Garnet-muscovite intergrowths, for example, have been reported to occur in granite pegmatites of the Bergell area, Italy (WENGER and ARMBRUSTER, 1991). These textures result from the simultaneous crystallization of the two minerals but are not necessarily the result of eutectic crystallization (e.g., TOMKEIEFF, 1983); they could also be interpreted as a product of cotectic crystallization, i.e., simultaneous crystallization of the two minerals over a certain temperature interval. To our knowledge, only ROY (1935) reported an interpretation of garnet-quartz intergrowths; in his view, the intergrowths in the studied samples from India were formed through eutectic crystallization.

This paper describes the occurrence of garnet-quartz intergrowths in pegmatites from three localities in Italy – Sivigia and Val Bona (both at Bergell) and Val Caffaro (Adamello). We present electron microprobe data for garnet and other minerals, preliminary oxygen isotope data, whole-rock chemical compositions, and results obtained by X-ray texture goniometry. These data will be used to discuss the possible formation mechanism of the intergrowths.

2. Geologic Setting

2.1. BERGELL

The Bergell pluton, located in the Central Alps, is composed primarily of a medium-grained, 32 Ma old tonalite at the margin and a coarse-grained, 30 Ma old granodiorite in the core (Fig. 1; VON BLANCKENBURG, 1992). It is in contact with various nappes at the transition between the Penninic and the Austroalpine realms (for details, see SCHMID et al. 1996): to the west, the Bergell pluton is underlain by the structurally lower Gruf Complex, which is composed predominantly of migmatitic gneisses and which, together with the lower Penninic Adula nappe, represents the distal European margin, originally situated north of the N-Penninic suture; the Gruf Complex and parts of the Bergell pluton are crosscut by the 25 Ma (KÖPPEL and GRÜNENFELDER, 1975; HANSMANN, 1996) old Novate granite, a garnet-bearing two-
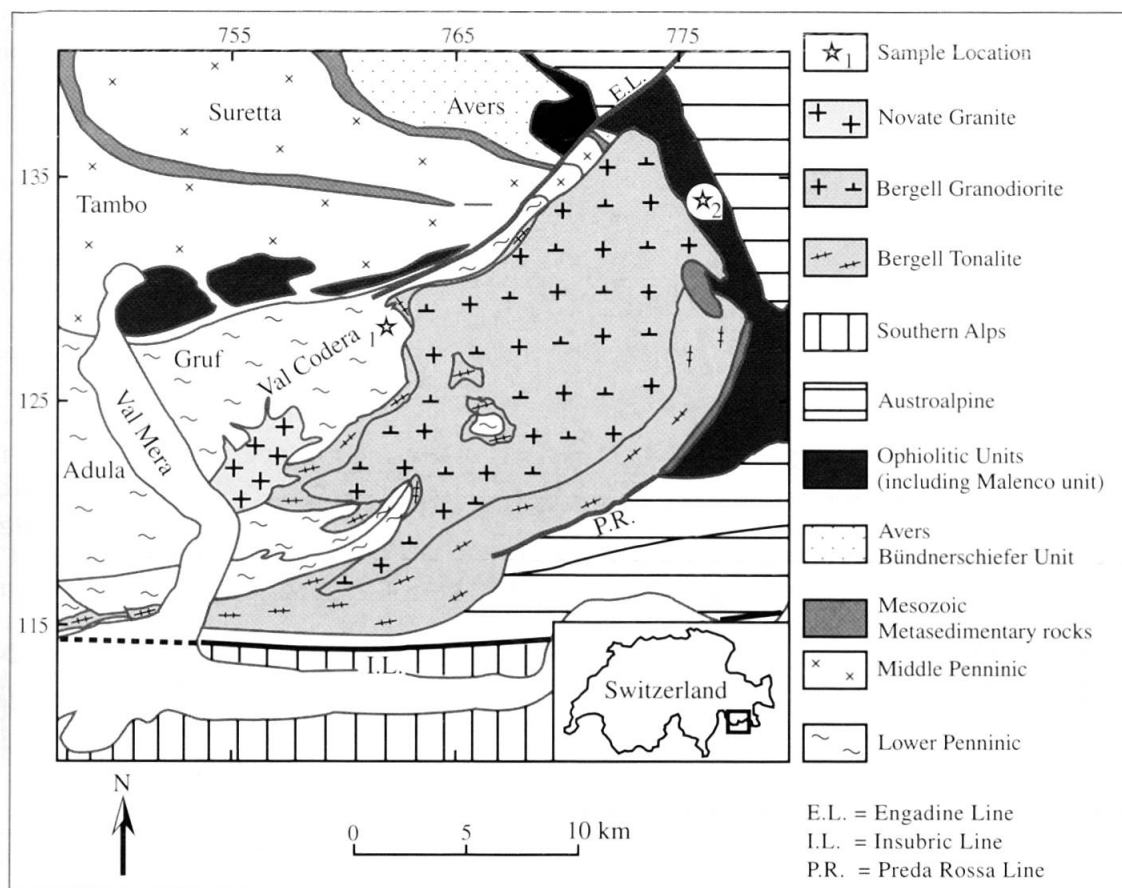
Fig. 1 Tectonic map of the Bergell region in the Central Alps (adapted from SCHMID et al., 1996).

mica granite stock which is associated with a system of dikes and is not genetically related to the Bergell pluton (REUSSER, 1987; VON BLANCKEN-BURG et al., 1992). To the east and northeast, the pluton is surrounded by the middle Penninic Tambo and Suretta nappes, representing the Briançonnais realm; the Forno unit, an ocean floor sequence from the S-Penninic suture zone; the Malenco unit, an exhumed segment of the crust-mantle boundary; and the lower Austroalpine Margna nappe, which was derived from the Apulian continental margin (SCHMID et al., 1996). All the units at the eastern margin of the Bergell have been overprinted by contact metamorphism (TROMMSDORFF and NIEVERGELT, 1985). Final emplacement and crystallization of the Bergell pluton occurred during a regional deformation event which is related to late-stage N-S shortening of the Alpine orogen and produced folding of the pluton floor as well as regional E-plunging stretching lineations in the country rocks (DAVIDSON et al., 1996).

Granitic pegmatites are found throughout the Bergell Alps. These youngest igneous rocks contain various amounts of alkali feldspar (often as coarse perthite), biotite, muscovite, plagioclase, and quartz, and are frequently characterized by a graphic texture. Some pegmatites, particularly the muscovite pegmatites, may further carry garnet, beryl, tourmaline, and a whole suite of rare minerals (GIERÉ, 1984; WENGER and ARMBRUSTER, 1991). The pegmatite dike near Sivigia, upper Val Codera (Italy) intruded into migmatitic gneisses of the Gruf complex, in close vicinity to the northwestern margin of the Bergell pluton (Fig. 1). The country rocks of the dike comprise two distinct migmatitic gneisses, a biotite-plagioclase-alkali-feldspar gneiss and a hypersthene- and hornblende-bearing biotite-labradorite-gneiss (the so-called Sivigia unit). The granitic dike is approximately 5 m wide, and can be followed along its strike (approximately NE–SW) for several hundred meters (see map of WENK and CORNELIUS, 1977). The samples studied here were collected from the core zone of this pegmatite dike (about 2 m from its contact with the country rocks, Swiss coordinates: 763.500/129.140). The second set of samples was collected from a pegmatite dike which cross-cuts the Bergell granodiorite in Val Bona, in the northeastern part of the Bergell pluton (Fig. 1, Swiss coordinates: 776.300/132.840). These samples have been studied previously by GIERÉ (1984).
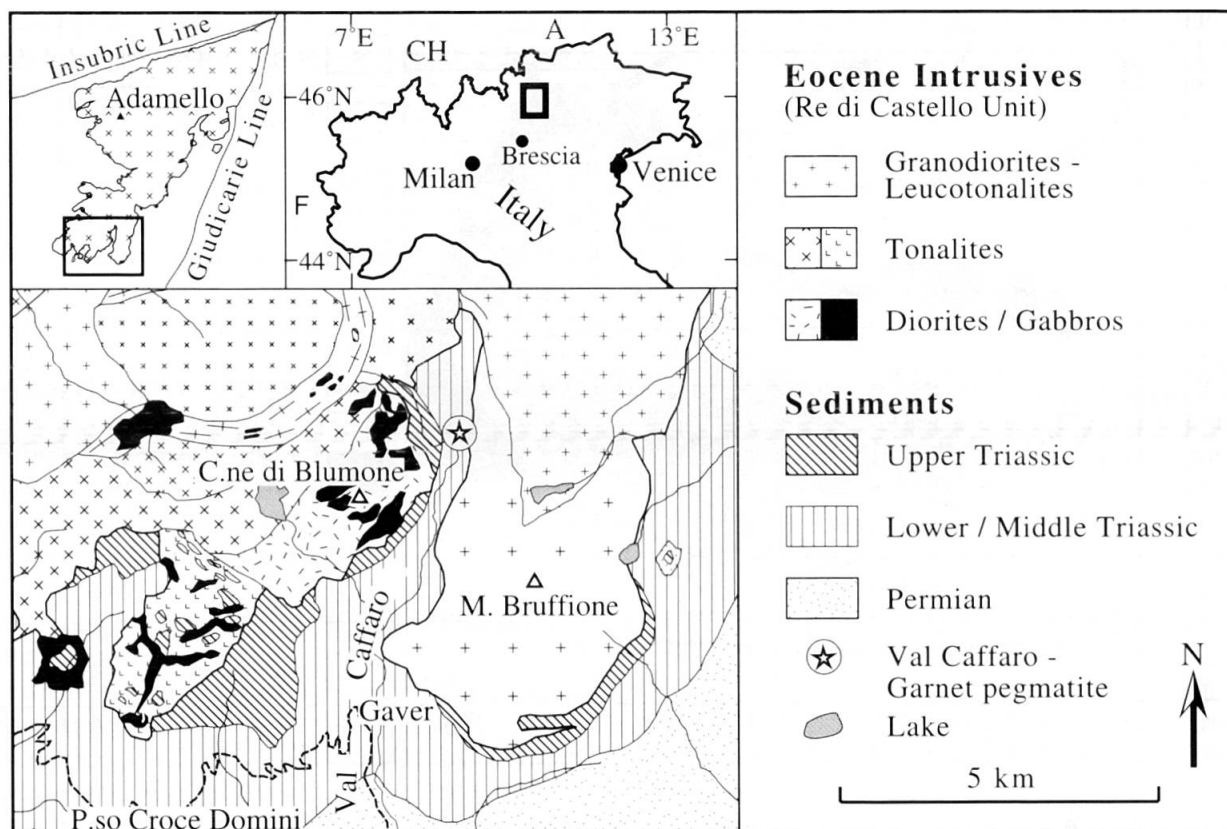
Fig. 2   Geological sketch map of the southern Adamello area in northern Italy, with indicated location in Val Caffaro of the sampled pegmatite on the western border of the Bruffione intrusion.

2.2. ADAMELLO

The Adamello batholith is the largest igneous complex of Tertiary age in the Alps. It is composed of several distinct granitoid plutons and numerous subsidiary mafic intrusions (BIANCHI et al., 1970; BRACK, 1984; CALLEGARI, 1985). These plutons were emplaced into schists and gneisses of the Southern Alpine basement and its cover of Permo-Mesozoic sedimentary rocks. DEL MORO et al. (1985) documented a systematic progression of emplacement age from the oldest plutons in the south (42 Ma) to the youngest plutons in the north (29 Ma). The Adamello massif shows many of the characteristic features of calc-alkaline cordilleran intrusions, which are dominated by hornblende-biotite-bearing metaluminous tonalites and granodiorites (BRACK, 1984, 1985; KAGAMI et al., 1991; ULMER et al., 1985). The southernmost and oldest pluton (CALLEGARI and DAL PIAZ, 1973; HANSMANN and OBERLI, 1991), the Re di Castello massif, forms itself a composite intrusion of predominantly gabbroic, tonalitic and granodioritic rocks, and is bordered by small mafic and ultramafic bodies (ULMER et al., 1985, BLUNDY and SPARKS, 1992).

The studied samples are from a pegmatite dike occurring in an outcrop located 250 m to the east of Casinetto di Blumone, Alta Val Caffaro (Fig. 2, Italian coordinate grid: 614.630/5090.950; 2340 m above sea level). The dike originates in the Bruffione granodiorite, gradually changes into a pegmatite consisting of quartz, alkali feldspar, albite and some biotite, and finally becomes a biotite-free pegmatite. This biotite-free pegmatite contains the studied garnet-quartz intergrowths and cross-cuts Middle Triassic metasediments, which in the outcrop are represented by metamorphosed interbedded limestones and marls of the Calcare di Angolo formation.

3. Petrographic Features

All three granitic pegmatite dikes are petrographically very similar. They contain macroscopic garnet-quartz intergrowths, many of which are nodule-shaped with well-defined boundaries (Fig. 3). These nodules are composed exclusively of garnet and quartz which are intimately intergrown. The pegmatite matrix consists of alkali feldspar, plagioclase, quartz, muscovite, some biotite (only at Bergell), and accessory minerals. Regular intergrowths of quartz and muscovite (Fig. 3d), and quartz and alkali feldspar (Fig. 4) are often observed in the matrix at all three localities.

Quartz varies in size from 0.005 to 1 mm, and is characterized by deformation features such as undulatory extinction, subgrains, cracks and dynamically recrystallized grains. These features are particularly prominent at Sivigia. Garnet, in which fractures are also observed (Figs 3c, 3f, 4b, 4c), is predominantly a spessartine-almandine solid solution (see Tab. 1, and below). Alkali feldspar shows the crosshatched twinning characteristic of microcline, contains albite exsolution lamellae (Tab. 2), and is commonly altered. Plagioclase has albite composition (Tab. 2), exhibits polysynthetic twinning, and is like alkali feldspar often slightly altered. In the Sivigia pegmatite, the twin lamellae are in many cases displaced along straight microfractures. Deformation is also documented by kinked cleavage planes in both muscovite (Mn-poor) and biotite (Mn-enriched), e.g., in the Val Bona pegmatite, biotite contains an average of 1.74 wt% MnO (Tab. 3). Magnetite (Tab. 4) and zircon occur as accessory minerals, except for the Val Bona locality, where magnetite is absent. In the Adamello pegmatite, two additional accessory phases were found: a brown mineral tentatively identified as yttrocolumbite-(Y), and pyrophanite (Tab. 4). The latter is significantly less abundant than magnetite and occurs as a thin rim around magnetite.

The microstructural observations indicate that all three pegmatites were subjected to minor postmagmatic solid-state deformation. Deformation was clearly most pronounced at the Sivigia locality. Postmagmatic deformation of the Bergell pluton has also been observed by other authors, particularly in the western and southern parts of the intrusion (BERGER et al., 1996).

4. Garnet-quartz intergrowths

4.1. BERGELL

The garnet-quartz intergrowths at Bergell exhibit some textural variation. In the middle of the largest nodule from Sivigia (approximately 7×5 cm in size), for example, thin bands of quartz and garnet (0.5–1.5 mm wide) are aligned nearly parallel to one another; in the outer parts, however, the intergrowth pattern is irregular (Figs 3a, 3b).

The composition of garnet is characterized by high Mn and Fe contents and only minor Mg and Ca contents (Tab. 1). At Sivigia, the contents of spessartine and pyrope are higher than at the Val Bona locality. Five electron microprobe traverses have been made across an entire garnet-quartz nodule of one sample from Sivigia (BV4b), and nine additional areas in the same sample were

chosen for more detailed analysis (Fig. 5a). The average end-member compositions of garnet in these areas are listed in table 5, and the average spessartine content is shown in figure 5a. The average spessartine content is highest in the center right part of the intergrowth (Area 4, near edge of the thin section), and decreases across the nodule with increasing distance from Area 4. Lowest spessartine contents are found along the left margin of the nodule in figure 5a, indicating that the nodule might exhibit an overall concentric zoning which, however, is truncated at the edge of the thin section.

Chemical zoning is not only observed on the nodule scale, but also on the scale of individual garnet lamellae within the intergrowths. A manganese distribution map is shown in figure 5b where the gray and black areas represent Mn-rich garnet and quartz, respectively; the X-ray maps for Mg, Ca and Fe look very similar. Thus, the chosen conditions for X-ray mapping were not sensitive enough to unveil chemical zoning of garnet in the studied part of the intergrowth. Quantitative electron probe microanalysis, on the other hand, revealed that of the 69 individual garnet lamellae analyzed in samples BV4a and BV4b, 35 lamellae show normal zoning, i.e., spessartine-rich central part and almandine-rich rim (see Fig. 6a), and 10 exhibit only weak zoning[1]; the remaining 24 lamellae are unzoned (Fig. 6b). Garnet lamellae with normal zoning occur both in the center and at the margins of the nodule (Areas 2, 4, 5, 7, 8, and 9 in Fig. 5a). The composition of the homogeneous lamellae is almost identical to that of the rims of the zoned lamellae (see Figs. 6a, 6b), indicating that the unzoned lamellae may have formed at the same time as the rims of the zoned lamellae, i.e., later than the Mn-rich central parts. In contrast to the Sivigia samples, garnet does not exhibit compositional zoning in the Val Bona pegmatite (Tab. 1).

4.2. ADAMELLO

In the garnet-quartz nodules from the Adamello pegmatite, the intergrowth pattern is quite regular, and in some parts, parallel garnet lamellae alternate with quartz (Fig. 3e). Most lamellae are less than 0.1 mm wide, but a few may be up to 0.5 mm in width. Some areas within garnet are much darker in color than others (Fig. 3f). These darker

---

[1] The term 'zoning' refers to the chemical variation observed in profiles along the short axis of the elongate garnet lamellae, i.e. in cross-sections rather than longitudinal sections.
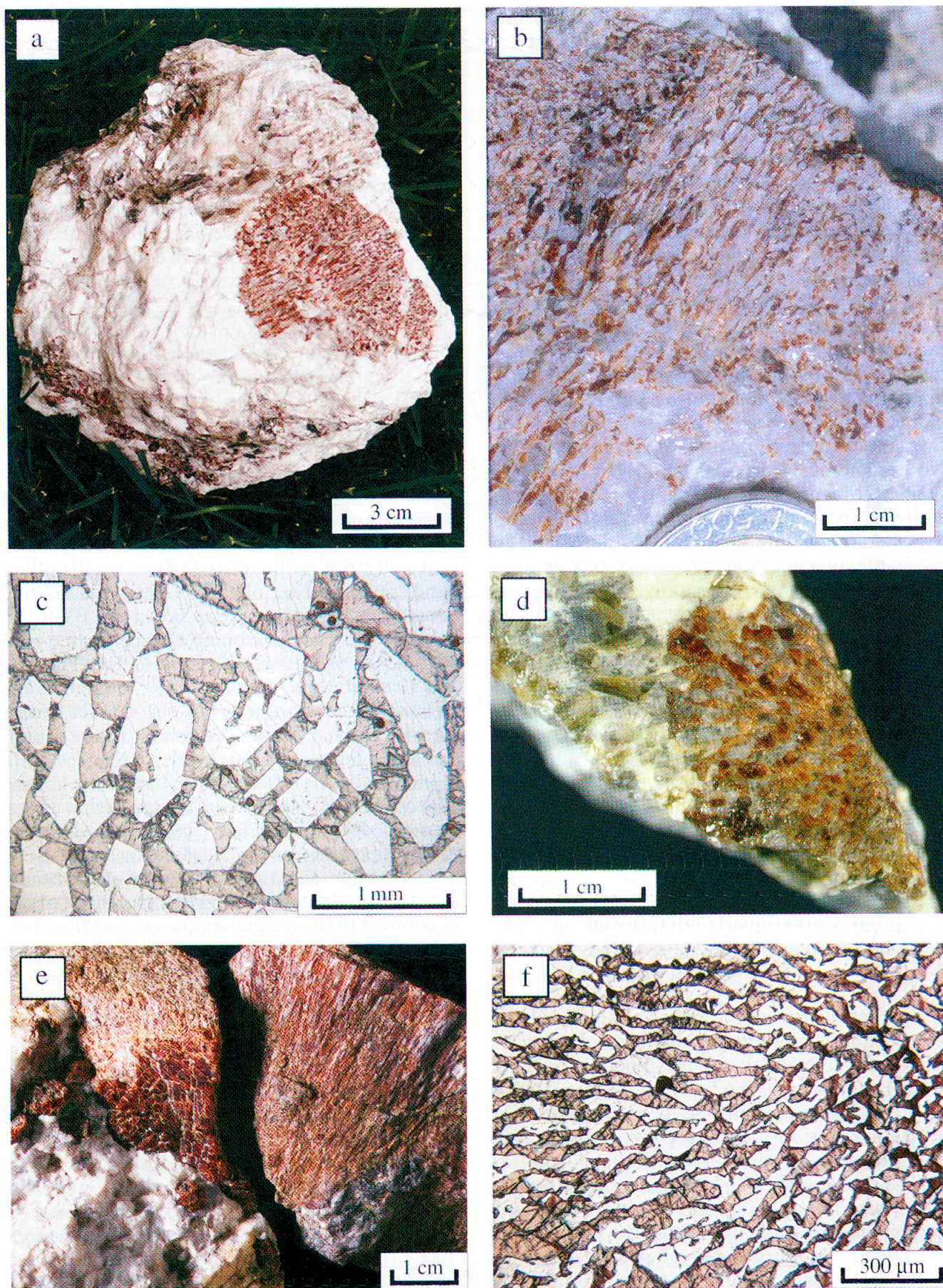
Fig. 3
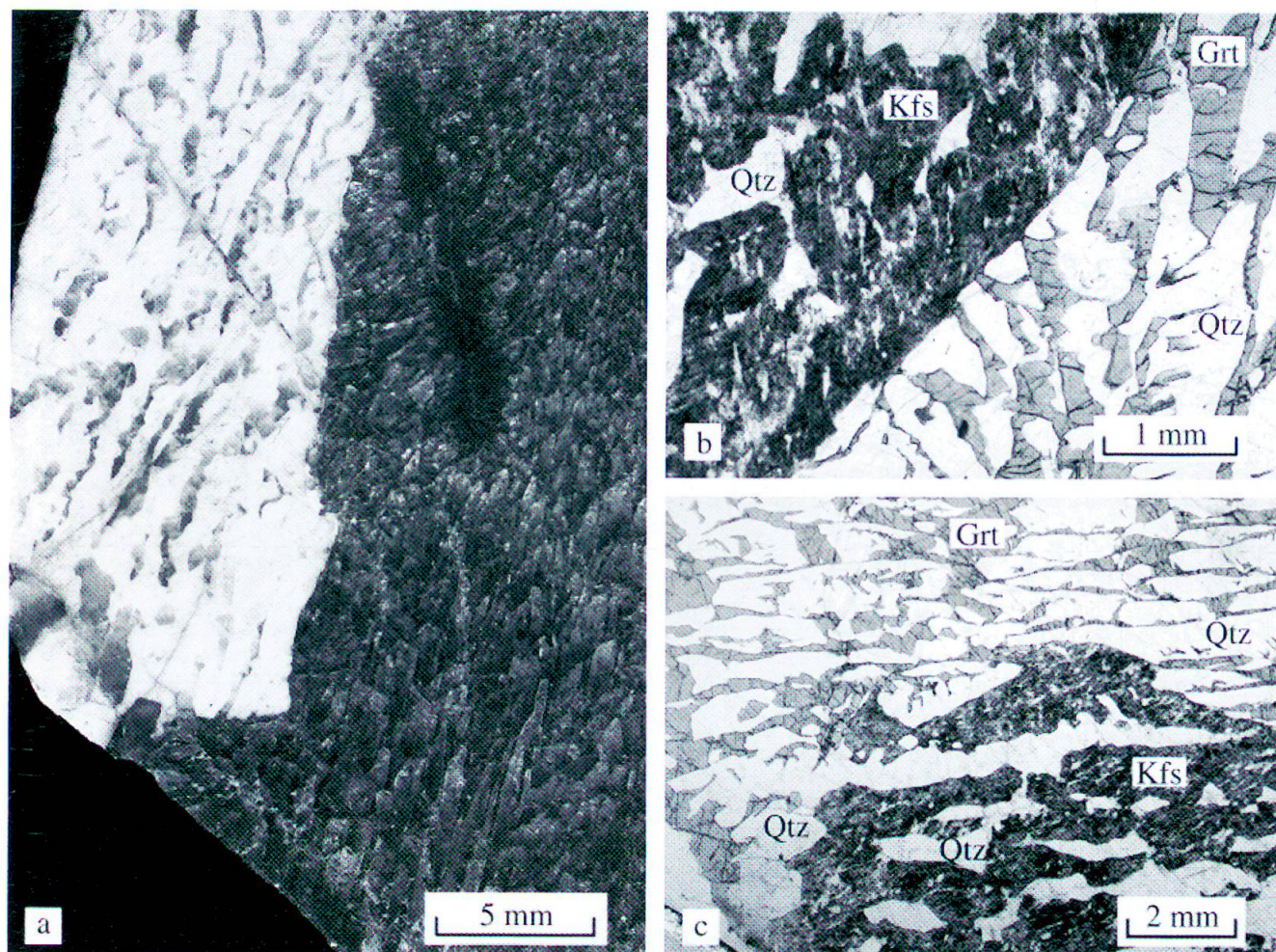
Fig. 4 Photographs of the boundary between the garnet-quartz intergrowth and the pegmatite matrix of the Val Caffaro locality, Adamello (sample 269a). (a) Boundary on the scale of the hand specimen; polished rock slab in daylight. (b) Digital photomicrograph of the sharp boundary where quartz does *not* penetrate into the alkali feldspar; plane polarized light. (c) Digital photomicrograph of the boundary where quartz can be followed without interruption from the garnet-quartz nodule into the graphic alkali feldspar-quartz intergrowth; plane polarized light. The matrix alkali feldspar (microcline perthite) contains abundant, small and narrow albite lamellae (light-colored) and appears dark due to alteration. Abbreviations: *Grt* = garnet, *Kfs* = alkali feldspar, *Qtz* = quartz.

areas occur as bands of variable width and with straight boundaries, but cannot be observed over the entire nodule. The optical zoning is typically discordant to the garnet/quartz grain boundaries, and the color bands can be followed across several neighboring lamellae (Fig. 7).

The Adamello garnet is, like in the Bergell pegmatites, a spessartine-almandine solid solution, but overall, its Mn content is higher than at Bergell (Tab. 1). For the coarse lamellae, the dark-colored areas are significantly richer in spessartine, but poorer in almandine, pyrope, and grossular than the light-colored areas. For the thinner lamellae, however, the average MnO contents of the dark areas are very similar to those of light-colored parts of garnet, and both are comparable to that of the coarse dark-colored garnet. Therefore, the color difference probably cannot be attributed to a single major chemical component, and must be related to some

← *Fig. 3* Hand specimen and thin section photographs of garnet-quartz intergrowths in pegmatites from Bergell and Adamello, Italy. (a) Sample BV4 from the Sivigia pegmatite, Bergell. (b) Detail of the garnet-quartz nodule shown in Figure 3a. (c) Digital photomicrograph showing a part of the garnet-quartz intergrowth of sample BV4b, plane polarized light. (d) Sample from the Val Bona pegmatite, Bergell. Note the muscovite-quartz intergrowth in upper left part of the sample. (e) Sample from Val Caffaro, Adamello. (f) Digital photomicrograph of Adamello thin section AU18A, plane polarized light.

Tab. 1 Representative electron microprobe analyses (in wt%) of garnet in the pegmatites from Bergell and Adamello, Italy.

Analysis #	Sivigia (Bergell) 1	2	3	4	5	Val Bona (Bergell) 1	2	3	Val Caffaro (Adamello) CD 1	CD 2	Mean(*)	CL 1	CL 2	Mean(*)	TD 1	Mean(*)	TL 1	Mean(*)
SiO₂	35.8	35.8	35.6	35.4	35.1	36.2	35.8	34.8	34.8	34.7	34.9(7)	34.8	35.8	35.2(6)	34.9	35.0(2)	34.8	34.8(6)
TiO₂	n.a.	n.a.	n.a.	n.a.	n.a.	0.08	0.05	0.07	0.20	0.15	0.18(4)	0.13	0.14	0.12(5)	0.21	0.18(4)	0.25	0.21(7)
Al₂O₃	20.3	20.2	20.1	20.1	19.9	20.5	20.7	20.7	19.9	20.0	19.9(2)	20.5	20.4	20.5(2)	19.7	19.6(2)	19.7	19.7(2)
FeO total	19.6	19.5	18.9	18.0	17.1	21.8	21.6	21.5	12.6	14.1	14(2)	16.6	16.2	16.1(8)	11.9	13(1)	12.0	12(1)
Fe₂O₃ calc	3.0	3.1	4.1	3.9	4.7	1.3	2.2	3.8	4.2	3.9	3.8	3.9	2.0	2.8	3.8	3.6	4.9	4.4
FeO calc	16.9	16.7	15.2	14.5	12.9	20.6	19.7	18.1	8.9	10.6	10.1	13.1	14.5	13.6	8.5	9.7	7.6	7.6
MnO	22.8	23.1	24.3	24.9	26.5	20.6	21.3	21.4	31.0	29.0	30(2)	25.9	25.5	25.8(9)	31.6	30(2)	30.9	31(2)
MgO	1.11	1.11	1.04	0.98	0.78	0.25	0.25	0.26	0.25	0.36	0.3(2)	0.54	0.55	0.53(7)	0.17	0.2(1)	0.25	0.2(1)
CaO	0.57	0.45	0.38	0.39	0.42	0.43	0.43	0.45	0.48	0.52	0.51(8)	0.62	0.72	0.7(1)	0.51	0.52(6)	0.45	0.48(9)
P₂O₅	n.a.	n.a.	n.a.	n.a.	n.a.	0.24	0.22	0.28	n.a.	n.a.								
Y₂O₃	0.00	0.07	0.21	0.20	0.15	0.04	0.00	0.01	0.21	0.20	0.23(7)	0.30	0.35	0.3(1)	0.25	0.2(1)	0.94	0.8(2)
Sc₂O₃	n.a.	n.a.	n.a.	n.a.	n.a.	n.a.	n.a.	n.a.	0.03	0.02	0.03(3)	0.05	0.03	0.03(3)	0.03	0.03(2)	0.11	0.08(3)
Total	**100.5**	**100.4**	**100.9**	**100.3**	**100.4**	**100.3**	**100.6**	**99.9**	**99.9**	**99.5**	**99.7**	**99.8**	**99.9**	**99.5**	**99.6**	**99.3**	**99.9**	**99.4**
Atomic Proportions (normalized to 8 cations and 12 oxygens)																		
Si	2.928	2.933	2.913	2.913	2.896	2.978	2.949	2.888	2.894	2.893	2.905	2.884	2.954	2.917	2.913	2.922	2.907	2.913
Ti						0.005	0.003	0.005	0.013	0.010	0.011	0.008	0.009	0.007	0.013	0.012	0.016	0.014
Al	1.957	1.949	1.940	1.950	1.932	1.991	1.993	2.019	1.948	1.967	1.951	2.002	1.985	2.006	1.935	1.928	1.939	1.944
Fe³⁺	0.187	0.192	0.254	0.242	0.290	0.080	0.135	0.236	0.260	0.247	0.240	0.243	0.122	0.176	0.238	0.225	0.307	0.281
Fe²⁺	1.159	1.145	1.038	0.998	0.889	1.421	1.352	1.253	0.618	0.738	0.705	0.909	1.000	0.942	0.594	0.678	0.532	0.535
Mn	1.584	1.604	1.687	1.735	1.854	1.438	1.484	1.506	2.184	2.044	2.093	1.817	1.782	1.811	2.229	2.149	2.183	2.204
Mg	0.135	0.136	0.127	0.120	0.095	0.031	0.031	0.032	0.031	0.045	0.040	0.066	0.068	0.066	0.021	0.030	0.031	0.028
Ca	0.050	0.039	0.034	0.034	0.037	0.038	0.037	0.040	0.042	0.046	0.045	0.055	0.064	0.061	0.045	0.047	0.040	0.043
P						0.017	0.016	0.020										
Y	0.000	0.003	0.009	0.009	0.007	0.002	0.000	0.001	0.009	0.009	0.010	0.013	0.015	0.014	0.011	0.009	0.042	0.036
Sc									0.001	0.001	0.001	0.002	0.001	0.001	0.001	0.001	0.004	0.003
End-members (mol%)																		
Grossular	1.70	1.34	1.16	1.17	1.28	1.28	1.31	1.41	1.47	1.60	1.56	1.93	2.17	2.09	1.57	1.61	1.41	1.52
Pyrope	4.62	4.64	4.37	4.15	3.31	1.06	1.07	1.13	1.08	1.57	1.38	2.31	2.33	2.28	0.73	1.03	1.11	0.98
Almandine	39.57	39.12	35.88	34.46	30.83	48.52	46.59	44.26	21.41	25.61	24.36	31.77	34.14	32.56	20.47	23.26	18.81	18.79
Spessartine	54.11	54.80	58.27	59.92	64.34	49.08	51.02	53.19	75.73	70.91	72.34	63.52	60.83	62.58	76.86	73.80	77.20	77.45

FeO_total is the original microprobe data; Fe₂O₃ calc and FeO calc were calculated according to stoichiometry. For the Val Caffaro pegmatite, CD = coarse dark-colored lamellae (mean for n = 46), CL = coarse light-colored lamellae (mean for n = 66), TD = thin dark-colored lamellae (mean for n = 16), TL = thin light-colored lamellae (mean for n = 30). (*) Values in parentheses reflect 2σ-error of digits to their immediate left. Garnet analysis positions for Sivigia: 1, 2 – rim of nodule, lamella rims; 3, 4, 5 – core of nodule, where 3, 4 are from rim, 5 from core of same lamella.

Tab. 2 Average composition of feldspar (in wt%) in the pegmatites from Bergell and Adamello, Italy.

	Sivigia (Bergell)			Val Bona (Bergell)			Val Caffaro (Adamello)		
	Plagioclase	Microperthite		Plagioclase	Microperthite		Plagioclase	Microperthite	
		Kfs Host	Ab Lamellae		Kfs Host	Ab Lamellae		Kfs Host	Ab Lamellae
	Mean(*) (n = 77)	Mean(*) (n = 12)	Mean(*) (n = 20)	Mean(*) (n = 26)	Mean(*) (n = 8)	Mean(*) (n = 40)	Mean(*) (n = 21)	Mean(*) (n = 33)	Mean(*) (n = 12)
SiO_2	66.6(4)	64.3(1)	67.9(5)	66(2)	64.5(3)	67.8(5)	67.0(9)	64.9(9)	68.5(6)
TiO_2	0.01(2)	0.01(1)	0.01(3)	n.a.	n.a.	n.a.	0.01(4)	0.0(1)	0.02(5)
Al_2O_3	21.1(2)	18.4(1)	19.5(5)	21.0(7)	18.5(2)	19.3(4)	20.6(4)	18.4(4)	19.6(2)
FeO_{total}	0.02(3)	0.2(1)	n.a.	n.a.	n.a.	n.a.	0.03(4)	0.03(8)	0.02(3)
CaO	1.7(1)	<0.01	0.2(4)	1.6(6)	n.a.	0.2(2)	1.3(3)	<0.01	0.2(2)
Na_2O	10.8(2)	0.9(2)	11.5(3)	11.0(4)	1.0(4)	11.8(3)	11.0(2)	1.2(6)	11.7(2)
K_2O	0.2(2)	15.3(2)	0.2(2)	0.2(1)	15.1(5)	0.2(3)	0.2(2)	15.0(8)	0.2(3)
Rb_2O	n.a.	n.a.	n.a.	n.a.	0.54(2)	0.57(2)	n.a.	n.a.	n.a.
BaO	0.02(6)	0.07(9)	0.02(6)	n.a.	n.a.	n.a.	0.01(5)	0.1(3)	0.01(4)
Total	**100.6**	**99.2**	**99.3**	**99.8**	**99.6**	**99.8**	**100.2**	**99.6**	**100.4**
Atomic Proportions (Normalized to 5 Cations and 8 Oxygens)									
Si	2.906	2.993	2.986	2.894	3.001	2.976	2.931	3.002	2.979
Ti	0.000	0.000	0.000				0.001	0.001	0.001
Al	1.086	1.008	1.012	1.088	1.015	1.001	1.062	1.004	1.007
Fe^{2+}	0.001	0.006					0.001	0.001	0.001
Ca	0.080	0.000	0.011	0.075	0.000	0.010	0.060	0.000	0.012
Na	0.913	0.085	0.979	0.935	0.086	1.002	0.932	0.104	0.989
K	0.014	0.907	0.012	0.009	0.898	0.011	0.014	0.886	0.013
Rb					0.016	0.016			
Ba	0.000	0.001	0.000				0.000	0.002	0.000
End-members (mol%)									
Orthoclase	1.37	91.36	1.18	0.85	89.78	1.01	1.38	89.33	1.30
Albite	90.64	8.52	97.68	91.80	8.60	96.43	92.62	10.45	97.55
Anorthite	7.96	0.00	1.11	7.35	0.00	1.00	5.99	0.00	1.13
Celsian	0.03	0.12	0.03				0.02	0.22	0.02
Rb-microcline					1.63	1.56			

Kfs = K-feldspar; Ab = Albite; n.a. = not analyzed.
(*) Values in parentheses reflect 2σ-error of digits to their immediate left.

trace elements. It is noteworthy that the Y_2O_3 content of the light-colored parts of garnet is, in most cases, higher than that of the dark-colored counterparts. Hence, the Y_2O_3 content may be one of the factors contributing to the color patterns in garnet.

Except for the mentioned parallel compositional and color bands, the chemical zoning across individual garnet lamellae at Adamello is similar to that observed at Sivigia. Most compositional profiles along cross-sections through individual garnet lamellae show normal zoning irrespective

Tab. 3   Average composition of micas (in wt%) in the pegmatites from Bergell and Adamello, Italy.

	Sivigia (Bergell)		Val Bona (Bergell)		Val Caffaro (Adamello)
	Muscovite	**Biotite**	**Muscovite**	**Biotite**	**Muscovite**
	Average(*) (n = 44)	Average(*) (n = 23)	Average(*) (n = 59)	Average(*) (n = 28)	Average(*) (n = 11)
SiO_2	45.2(3)	35.2(5)	45.5(6)	34(1)	45.2(7)
TiO_2	0.2(1)	1.7(2)	n.a.	2.4(4)	0.2(2)
Al_2O_3	33.5(4)	17.9(6)	35.0(8)	17.4(5)	33(1)
FeO total	4.0(3)	21.7(7)	2.4(7)	24.6(6)	4.1(4)
Fe_2O_3 calc	4.27		2.46		2.06
FeO calc	0.12		0.18		2.27
MnO	0.04(4)	1.06(6)	(**)	1.7(3)	0.2(2)
MgO	0.72(9)	8.3(6)	0.43(7)	5.5(4)	0.2(5)
CaO	n.a.	0.02(3)	n.a.	n.a.	n.a.
Na_2O	0.7(2)	0.15(7)	0.8(2)	n.a.	0.32(8)
K_2O	10.4(3)	9.4(1)	10.2(3)	9(1)	10.6(3)
Rb_2O	n.a.	0.17(2)	0.39(2)	0.31(2)	n.a.
F	< 0.03	< 0.03	n.a.	0.8(3)	<0.03
H_2O calc	4.45	3.80	4.46	3.71	4.40
O = F				0.33	
Total	**99.7**	**99.4**	**99.4**	**99.9**	**99.0**
Atomic Proportions (Normalized to 20 oxygens, 4 (OH, F), and 14 cations for muscovite or 16 for biotite)					
Si	6.089	5.550	6.113	5.439	6.165
Ti	0.023	0.204	0.000	0.283	0.020
Al	5.319	3.328	5.547	3.232	5.347
Fe^{3+}	0.433		0.249		0.212
Fe^{2+}	0.013	2.859	0.020	3.238	0.259
Mn	0.005	0.141		0.233	0.022
Mg	0.144	1.958	0.085	1.291	0.049
Ca		0.003			
Na	0.182	0.047	0.195		0.086
K	1.794	1.892	1.758	1.861	1.842
Rb		0.017	0.034	0.031	
F				0.391	

(*) Values in parentheses reflect 2σ-error of digits to their immediate left.
(**) No Mn peak was detected in a wavelength dispersive spectrum and therefore, Mn was not analyzed quantitatively.
n.a. = not analyzed. Fe_2O_3 calc, FeO_{calc}, and H_2O were calculated according to stoichiometry.
No biotite was observed in the Val Caffaro pegmatite.

of thickness and color (e.g., Fig. 6c). Some lamellae exhibit only weak zoning, and others are homogeneous (e.g., Fig. 6d).

5. X-Ray Texture Goniometry

One garnet-quartz nodule from Sivigia has been studied by X-ray texture goniometry. The results

Tab. 4   Average composition of opaque minerals (in wt%) in the pegmatites from Bergell and Adamello, Italy.

	Sivigia (Bergell)	Val Caffaro (Adamello)	
	Magnetite	Magnetite	Pyrophanite
	Average(*) (n = 26)	Average(*) (n = 35)	Average(*) (n = 25)
SiO_2	0.07(6)	n.a.	n.a.
TiO_2	0.11(9)	0.6(4)	52.0(5)
Al_2O_3	0.07(8)	n.a.	n.a.
FeO_{total}	92.9(7)	93(1)	23(2)
$Fe_2O_{3\ calc}$	68.8	67.9	0.81
FeO_{calc}	31.1	31.5	21.98
MnO	0.25(9)	n.a.	24(2)
MgO	0.01(2)	n.a.	n.a.
CaO	0.01(3)	n.a.	n.a.
Total	**100.3**	**100.0**	**99.4**
Atomic Proportions			
	Normalized to 24 Cations and 32 Oxygens	Normalized to 24 Cations and 32 Oxygens	Normalized to 2 Cations and 3 Oxygens
Si	0.022		
Ti	0.025	0.127	0.992
Al	0.024		
Fe^{3+}	15.882	15.747	0.015
Fe^{2+}	7.973	8.127	0.466
Mn	0.064		0.526
Mg	0.006		
Ca	0.004		

(*) Values in parentheses reflect 2σ-error of digits to their immediate left.
n.a. = not analyzed. No magnetite was observed in the Val Bona pegmatite.

Tab. 5   Average end-member composition of garnet in Areas 1 to 9 (see Fig. 3a) in sample BV4b from the Sivigia pegmatite (in mol%).

Area #	1	2	3	4	5	6	7	8	9
End-member	Mean(*) (n=118)	Mean(*) (n=278)	Mean(*) (n=155)	Mean(*) (n=86)	Mean(*) (n=125)	Mean(*) (n=124)	Mean(*) (n=102)	Mean(*) (n=118)	Mean(*) (n=51)
Grossular	1.2(2)	1.2(1)	1.3(1)	1.2(1)	1.3(1)	1.3(1)	1.2(1)	1.2(3)	1.2(2)
Pyrope	4.0(5)	4.0(3)	3.7(3)	3.4(5)	3.6(5)	4.1(4)	4.0(3)	3.6(6)	3.3(3)
Almandine	38(1)	36(1)	35(2)	32(2)	33(2)	37(2)	36(1)	36(3)	35(2)
Spessartine	57(2)	58(1)	60(2)	63(2)	62(3)	58(2)	58(2)	58(3)	60(2)

(*) Values in parentheses reflect 2σ-error of digits to their immediate left.

suggest that within the analyzed area (4 × 10 mm), the nodule consists of a single garnet crystal which is intergrown with a single quartz crystal (Fig. 8). There is some deviation of the quartz orientation from that of an ideal single crystal due to the mentioned subgrain formation (visible in thin section). The c-axis of quartz is located at the center of the small circle distribution of positive and negative rhomb reflections ($10\bar{1}1$) of quartz in figure 8 (approximately in the center of the pole figure). The quartz c-axis is oriented between

the poles to (011) and (112) of the garnet grain. There is no obvious systematic intergrowth of garnet and quartz along specific crystallographic orientations of both minerals.

To obtain more textural information about the nodules in the Adamello pegmatite, we have performed X-ray texture goniometry for a garnet-quartz intergrowth in sample AU18A. Within the analyzed area (4 × 10 mm), the garnet consists of a single crystal, but the quartz is a polycrystalline aggregate. The pole figures (Fig. 8) show that quartz

Tab. 6   Oxygen isotope data for the Sivigia pegmatite (sample BV4).

Minerals	$\delta^{18}O_{SMOW}$ (‰)	$\delta^{18}O_{SMOW}$ (‰) Normalized XRAL values[2]	Mean $\delta^{18}O_{SMOW}$ (‰)
Quartz	11.5 ± 0.2	11.9 ± 0.2 (within intergrowth) 11.8 ± 0.2 (outside intergrowth)	11.7 ± 0.1
Plagioclase (An_8[1])	10.1 ± 0.2		10.1 ± 0.2
Muscovite	9.1 ± 0.2		9.1 ± 0.2
Garnet	8.4 ± 0.2	8.4 ± 0.2	8.4 ± 0.2

[1] The composition of plagioclase was determined by electron microprobe analysis (see Tab. 2).

[2] The original $\delta^{18}O$ values determined by XRAL Laboratories were 6.8, 10.3, and 10.2‰ for garnet, quartz within and quartz outside the garnet-quartz intergrowth, respectively. Normalized values calculated assuming identical $\delta^{18}O_{SMOW}$ values for garnet.

There was only one analysis for each mineral in these two groups of analyses.
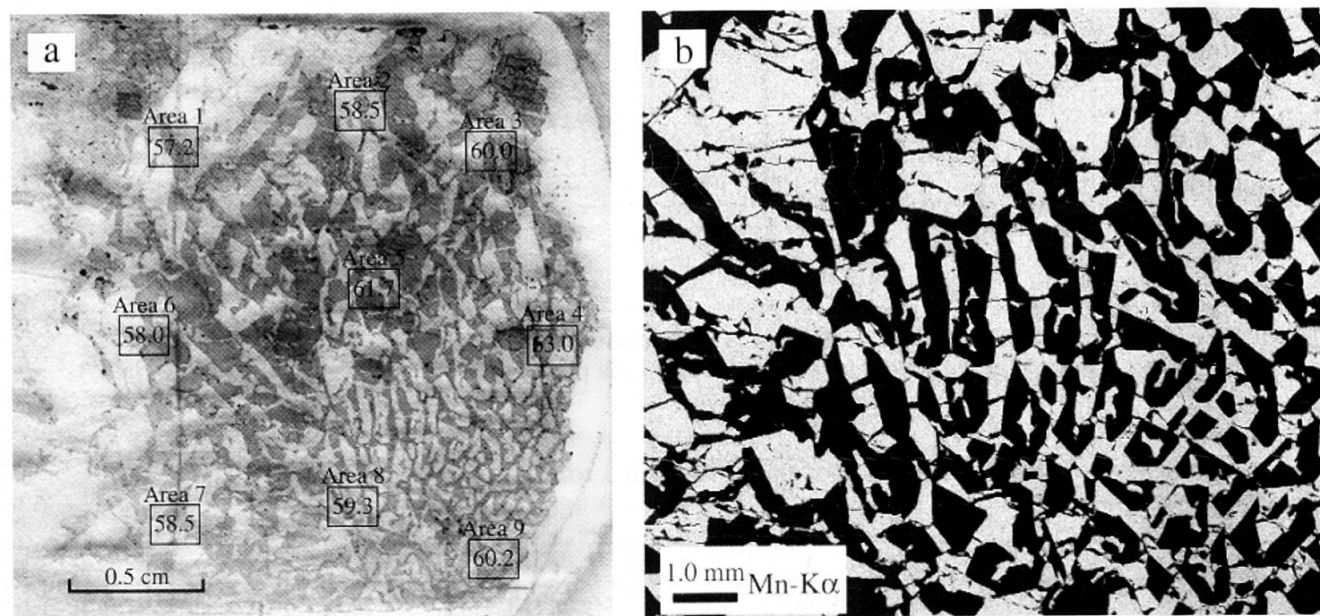
Notation: SMOW = Standard Mean Ocean Water.

Fig. 5   X-ray map and analysis areas of sample BV4b from Sivigia, Bergell. (a) Photograph of thin section BV4b used for garnet analysis, plane polarized light. Systematic electron probe microanalysis of garnet has been carried out inside the 9 rectangular areas (Areas 1 to 9), and the average spessartine contents (in mol%) are given in the corresponding areas (see table 2 for standard deviations). (b) X-ray map of a portion of the garnet-quartz intergrowth in sample BV4b, showing the distribution of Mn. Light colored-areas are Mn rich, black areas represent quartz and fractures/cracks. This X-ray map covers the lower right part of the garnet-quartz intergrowth shown in figure 5a.

does not exhibit any crystallographic preferred orientation (random orientation of comparatively low-strength maxima) or systematic crystallographic relationship with the single-crystal garnet.

6. Oxygen Isotopes

Oxygen isotopic compositions were determined for the major minerals in one of the pegmatite samples from Sivigia (sample BV4). A limited set of analyses is available for separates of garnet, quartz, plagioclase, and muscovite. No data were obtained for alkali feldspar because it was virtually indistinguishable from *untwinned* plagioclase under the stereomicroscope. The preliminary $\delta^{18}O$ values obtained for these minerals (Tab. 6) exhibit the normal sequence (EPSTEIN and TAYLOR, 1967; TAYLOR and EPSTEIN, 1962; ZHENG, 1993a), i.e., quartz > plagioclase > muscovite > garnet, and the differences between the $\delta^{18}O$ values of these minerals are within a normal range.
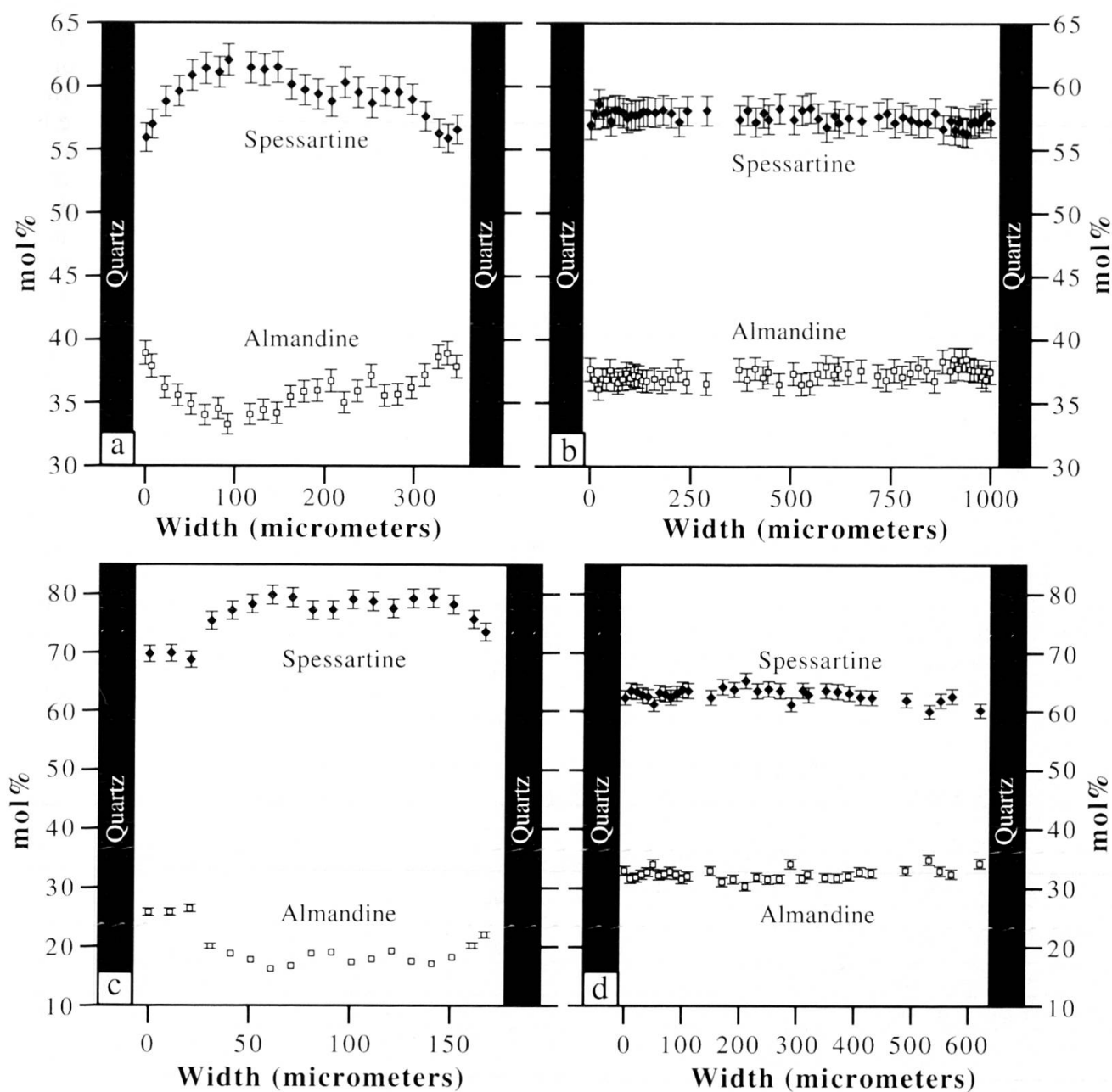

Fig. 6 Examples of compositional profiles along cross-sections through garnet lamellae within a garnet-quartz intergrowth in samples BV4b (Bergell) and AU18A (Adamello). (a) Profile across a garnet lamella in Area 8 of sample BV4b (Fig. 5a) exhibiting normal zoning. (b) Profile across an unzoned garnet lamella in Area 1 of sample BV4b (Fig. 5a). (c) Profile across a thin, light-colored garnet lamella showing normal zoning; sample AU18A (d) Profile across a coarse, light-colored garnet lamella with no zoning; sample AU18A. Error bars represent the 2σ-uncertainties resulting from counting statistics; some errors are smaller than symbol.
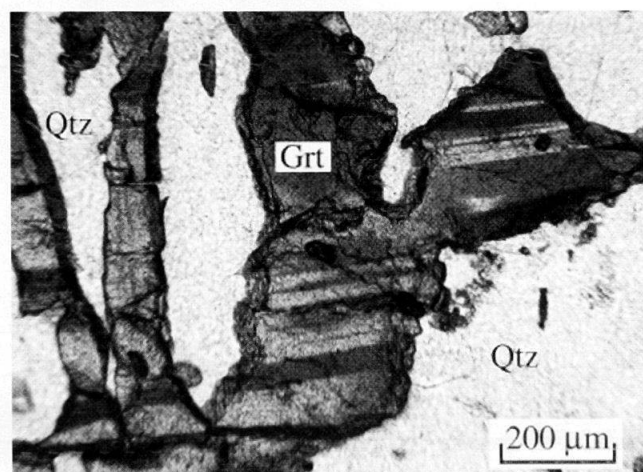
Fig. 7 Digital photomicrograph of a detail in the garnet-quartz nodule of the Val Caffaro pegmatite, Adamello. The alternating light and dark color zones in garnet are parallel, but discordant to the garnet/quartz grain boundaries, and can be traced across neighboring garnet lamellae. Sample AU18A, plane polarized light. Abbreviations: *Grt* = garnet, *Qtz* = quartz.

Additional analyses, performed by XRAL Laboratories (see Appendix), yielded $\delta^{18}O_{SMOW}$ values of 6.8, 10.3, and 10.2 ($\pm$ 0.2‰) for garnet, quartz within and quartz outside the garnet-quartz intergrowth, respectively. These data, although different in absolute values, agree quite well with our own analyses after normalizing with respect to the garnet sample (Tab. 6). There are two reasons for carrying out the normalization based on the $\delta^{18}O$ value of garnet obtained by us at Purdue University. First, the same garnet separate was analyzed in both laboratories, and thus, the $\delta^{18}O$ values should be the same. Secondly, we

used NBS-28 as actual standard, while XRAL Laboratories used a laboratory standard, calibrated relative to NBS-28.

The relatively high $\delta^{18}O$ values (> 10‰) of quartz and plagioclase, which are the dominant minerals besides microcline, suggest that the pegmatite from Sivigia has a bulk-rock $\delta^{18}O_{SMOW}$ value of approximately 10‰ or higher. This is similar to the value of 9.9‰ reported for another pegmatite dike occurring in the eastern Bergell (VON BLANCKENBURG et al., 1992). These values are significantly higher than those of both tonalite and granodiorite from the Bergell pluton ($\delta^{18}O_{SMOW}$ = 7.5–8.8‰ and $\delta^{18}O_{SMOW}$ = 9.1‰, respectively), and also higher than that of the Novate granite ($\delta^{18}O_{SMOW}$ = 9.1‰; DIETHELM, 1989; VON BLANCKENBURG et al. 1992). The high $\delta^{18}O_{SMOW}$ values for the Sivigia rocks indicate that the pegmatite melt may have been derived from metasedimentary rocks. Moreover, the fact that the $\delta^{18}O$ values of the constituent minerals are in normal sequence indicates that the pegmatite has not been subjected to extensive postmagmatic hydrothermal alteration.

The mean oxygen isotope data (Tab. 6) have been used to estimate the equilibration temperature between mineral pairs. The temperature for oxygen isotope equilibration between garnet and quartz was calculated at 717 ± 53 °C and 727 ± 47 °C using the thermometer of ZHENG (1993a) and a combined thermometer (MATTHEWS et al., 1983; ROSENBAUM and MATTEY, 1995), respectively (Tab. 7). This estimate is consistent with the temperature calculated for the plagioclase-garnet pair (768 ± 144 °C) using the oxygen isotope thermometer of BOTTINGA and JAVOY (1975). The average temperature obtained for the equilibration

Tab. 7 Results of oxygen isotope thermometry for the Sivigia pegmatite.

Mineral Pair	Applicable Temperature Range of Thermometer (°C)	T calculated (°C)	Reference used for calculations
Mean Quartz - Garnet	0-1200	717 ± 53**	ZHENG (1993a)
Mean Quartz - Garnet	Extrapolation*	727 ± 47**	MATTHEWS et al. (1983), ROSENBAUM and Mattey (1995)
Plagioclase (An$_8$) – Garnet	>500	768 ± 144**	BOTTINGA and JAVOY (1975)
Mean Quartz - Muscovite	>500	617 ± 48**	BOTTINGA and JAVOY (1973; 1975)
Mean Quartz - Muscovite	0-1200	600 ± 62**	ZHENG (1993b)

* This thermometer is derived from the quartz-calcite thermometer of MATTHEWS et al. (1983) and the garnet-calcite thermometer of ROSENBAUM and MATTEY (1995). The quartz-calcite thermometer was calibrated at 500–700 °C and 13.4 kbar, and the garnet-calcite thermometer was calibrated at 800–1200 °C and about 23 kbar using grossular/andradite garnet.
** The uncertainties are calculated from the maximum combined analytical errors. Two uncertainties were calculated (using the lower and upper limits of the $\delta^{18}O_{SMOW}$ differences between each pair of minerals), and the larger one is listed.

Bergell

Garnet (400) Quartz (10$\bar{1}$1)

Adamello

Garnet (400) Quartz (10$\bar{1}$1)
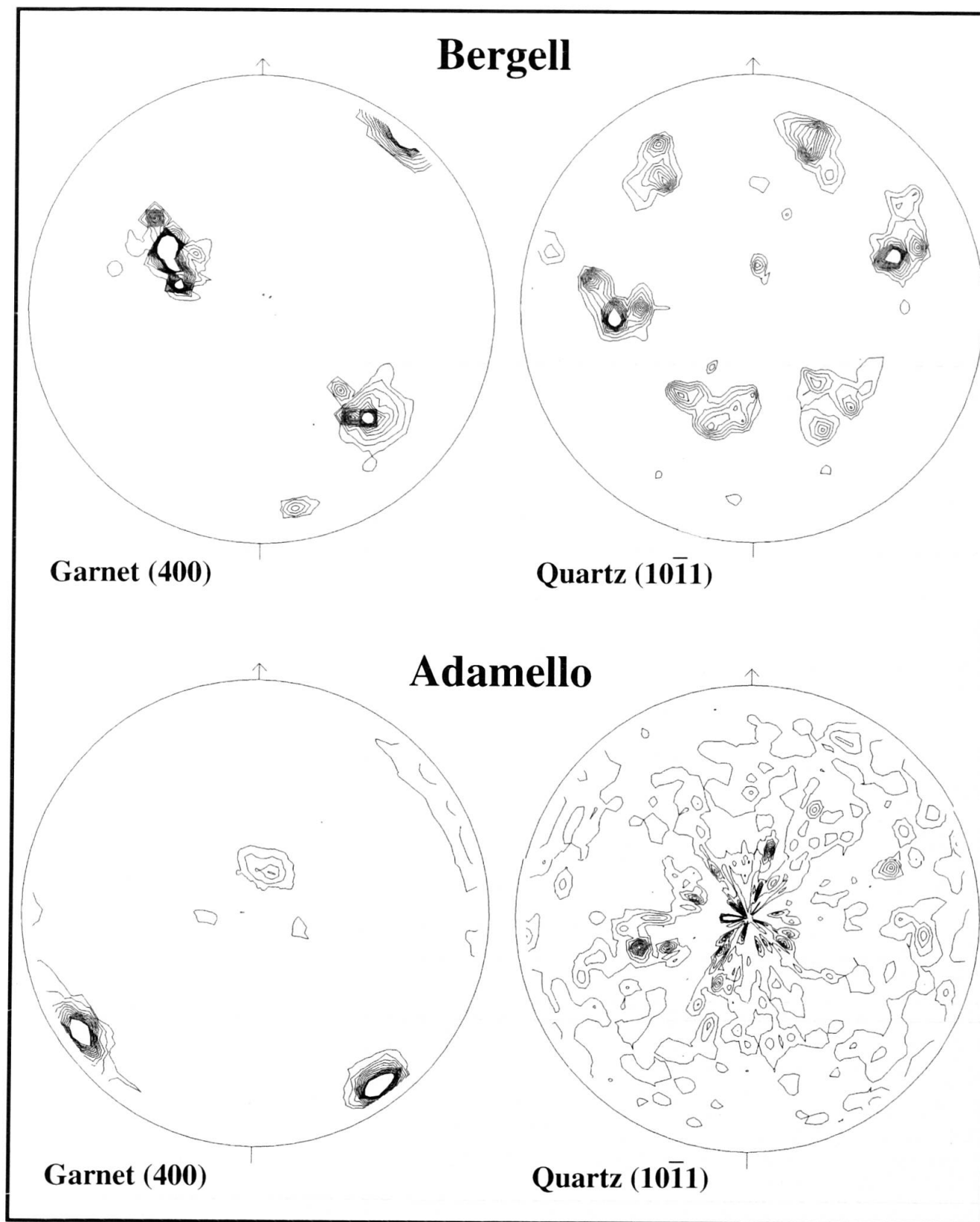
Fig. 8 Pole figures of the two garnet-quartz intergrowths (Bergell and Adamello) measured by X-ray texture gonio-metry. The diagrams for the Bergell sample show a single quartz crystal intergrown with a single garnet crystal, whereas the Adamello pole figures indicate a single garnet crystal intergrown with a polycrystalline quartz aggregate. Contour intervals are: 1-, 2-, 3-, 4-, 5-, 6-, 7-, 8-, 9-, 10-times uniform distribution for quartz, and 2-, 5-, 10-, 15-, 20-, 25-, 30-, 35-, 40-, 45-, 50-times uniform distribution for garnet.

Tab. 8 Bulk-rock composition of the studied pegmatites and other selected rocks from the Bergell area.

	Sivigia Pegmatite	Val Bona Pegmatite	Other Pegmatites			Novate Granite	Aplites	Leuco-granite	Bergell Tonalite	Bergell Grano-diorite	Gruf Complex Gneiss
Sample #	BV4	Peg1	Siss7	M-PNG1-P	M-P1						
Reference	this study	this study	1)	2)	2)	3), 5), 6), 7)	3), 4)	4)	3)	3)	3)
(wt%)	(n = 1)	(n = 1)	(n = 1)	(n = 1)	(n = 1)	Mean(*) (n = 7)	Mean(*) (n = 8)	Mean(*) (n = 7)	Mean(*) (n = 15)	Mean (n = 2)	Mean (n = 2)
SiO_2	73.3	73.8	75.57	75.81	69.96	73(2)	74(5)	75(1)	58(2)	68.13	67.61
TiO_2	0.03	0.05	0.05	0.06	0.07	0.09(5)	0.2(2)	0.2(1)	0.72(7)	0.37	0.43
Al_2O_3	13.9	14.7	14.29	14.63	16.66	15(2)	14(2)	14.6(6)	17.3(7)	15.55	16.29
Fe_2O_3	0.32	0.34	0.27	0.80[a]	1.21[a]	0.4(8)	0.2(3)	0.3(3)	2.0(9)	0.50	0.77
FeO	0.30	0.10	0.25	n.a.	n.a.	0.5(4)	0.7(9)	0.9(5)	4.5(8)	2.20	2.40
MnO	0.34	0.01	0.00	0.07	0.26	0.02(2)	0.02(4)	0.02(2)	0.12(2)	0.05	0.06
MgO	0.01	0.12	0.12	0.16	0.12	0(1)	0.2(4)	0.00(0)	3.5(4)	1.10	1.21
CaO	0.21	0.54	0.84	0.43	0.33	2(1)	1(1)	1.0(6)	7.0(7)	2.98	3.74
Na_2O	2.22	3.63	3.82	2.47	5.03	4.2(8)	4(1)	2(1)	3.1(6)	3.59	4.44
K_2O	7.66	5.28	4.28	4.33	3.48	4(1)	4(2)	5(1)	2.1(6)	4.21	1.69
P_2O_5	0.11	0.09	0.07	0.16	0.10	0.05(3)	0.09(9)	0.15(9)	0.21(7)	0.22	0.14
H_2O [b]	0.26	0.53	0.47	n.a.	n.a.	0.4(4)	0.4(4)	0.7(4)	1.2(2)	0.66	0.72
CO_2	n.a.	n.a.	n.a.	n.a.	n.a.	0.01(4)	0.1(4)	0.05(4)	0.05(4)	0.06	0.05
Total	**98.7**	**99.2**	**100.0**	**99.1**[c]	**97.3**[c]	**99.6**	**99.9**	**100.1**	**99.4**	**99.6**	**99.5**
Σ(Alkali) [d]	9.88	8.91	8.10	6.80	8.51	7.84	8.25	7.53	5.14	7.80	6.13
Al# [e]	1.13	1.16	1.15	1.53	1.32	1.07	1.08	1.29	0.86	0.98	1.02
Corundum [f]	1.84	2.24	2.04	5.51	4.38	1.12	1.53	3.67	0	0.31	0.82
Trace Element Content (ppm)											
Ba	< 20	< 20	94	< 10	< 10	794(260)	365(389)	322(368)	565(327)	664	497
Rb	325	468	178.1	391	930	103(110)	201(86)	158(63)	78(33)	154	39
Sr	16	17	48.38	16	<15	514(585)	160(164)	126(83)	299(68)	283	440
Nb	18	34	n.a.	34	93	< 9	7(5)	7(8)	< 9	< 9	< 9
La	3	3	4.5	n.a.	n.a.	< 4	15(21)	< 20	8(14)	< 4	9
Ce	7	7	8.6	n.a.	n.a.	< 13	28(39)	24(20)	44(28)	32	51
Nd	3	4	6.383	n.a.	n.a.	< 10	17(14)	< 25	14(10)	< 10	11
Y	14	8	10	32	28	4(3)	12(7)	11(8)	21(5)	8	7
Zr	43	420	17	72	37	47(41)	96(98)	56(61)	117(41)	123	133
V	n.a.	n.a.	<10	< 10	< 10	< 18	17(11)	< 10	178(30)	34	65
Cr	< 70	< 70	< 6	128	117	< 8	7(2)	6(1)	22(11)	11	19
Ni	n.a.	n.a.	< 3	10	18	< 4	6(8)	< 3	8(3)	< 4	6
Co	n.a.	n.a.	23	< 4	< 4	< 6	9(8)	11(10)	23(3)	7	14
Cu	n.a.	n.a.	< 3	< 3	< 3	< 7	6(4)	4(4)	12(12)	< 7	< 7
Zn	n.a.	n.a.	14	29	50	16(4)	20(22)	21(24)	62(7)	22	38
Ga	n.a.	n.a.	n.a.	27	48	13(4)	14(7)	13(4)	16(2)	10	15
Sc	n.a.	n.a.	3	3	< 2	< 3	3(1)	2(2)	23(6)	5	7
S	n.a.	n.a.	< 50	n.a.	n.a.	<100	81(48)	60(50)	< 100	< 100	< 100
Pb	n.a.	n.a.	n.a.	24	18	15(9)	n.a.	n.a.	< 10	13	< 10
Th	5	5	6.5	31	24	< 8	n.a.	6.1	< 8	< 8	< 8
U	36	10	7.00	36	24	< 20	n.a.	1.9	< 20	< 20	< 20

The Sivigia and Val Bona Pegmatite samples were analyzed by XRAL laboratories using XRF, except for Y, Th, and U (ICPMS), and FeO (titration). The detection limit of major elements listed as oxides was 0.01 wt% except for TiO_2, whose detection limit was 0.001 wt%. The detection limit of Ba was 20 ppm, that of Y 1ppm, those of Th and U 0.1 ppm, and those of the other trace elements 2 ppm. n.a. = not analyzed. (a) Value represents total iron content. (b) Calculated from Loss on Ignition and determinations of Fetot and FeO. (c) Includes 0.17 wt% and 0.10 wt% Loss on Ignition for M-PNG1-P and M-P1, respectively. (d) Σ(Alkali) = Na_2O + K_2O (wt%). (e) Al# = Al_2O_3/(Na_2O+K_2O+CaO); Al_2O_3, Na_2O, K_2O and CaO in moles. (f) Corundum is CIPW normative corundum in wt%. (*) Values in parentheses reflect 2σ-error of digits to their immediate left. References: 1) VON BLANCKENBURG et al. (1992); 2) WENGER and ARMBRUSTER (1991); 3) REUSSER (1987); 4) DIETHELM (1989); 5) MOTICSKA (1970); 6) WENK et al. (1977); 7) HAFNER (1993).

between muscovite and quartz (BOTTINGA and JAVOY, 1973; BOTTINGA and JAVOY, 1975; ZHENG, 1993b), however, is approximately 100 degrees lower than that obtained from the garnet-quartz pair (Tab. 7).

7. Whole-Rock Chemical Composition

The pegmatites from Sivigia and Val Bona were further investigated with respect to their whole-rock chemical composition. These two pegmatites are characterized by a high total alkali content, which is higher than in any other igneous rocks from the Bergell area (Tab. 8). Another characteristic of these and other garnet-bearing muscovite pegmatites (samples M-PNG1-P, M-P1), is that these rocks are all richer in Rb, Nb and U, but significantly poorer in Ca, Sr and Ba than the other intrusive rocks. The Aluminum numbers (Al#) of the Sivigia and Val Bona pegmatites (1.13 and 1.16, respectively) are identical to that of another muscovite pegmatite from the Bergell area which, however, does not contain garnet (sample Siss7, Tab. 8). Higher Al# are only exhibited by two other garnet-bearing muscovite pegmatites from the Eastern Bergell (samples M-PNG1-P, M-P1) and by the leucogranites, most of which occur in

upper Val Codera in the vicinity of the Sivigia pegmatite. These leucogranites typically contain both muscovite and biotite and, in some outcrops, additionally garnet (DIETHELM, 1989). Because the Al# of all pegmatites and leucogranites of the Bergell are greater than 1.1, they can be classified as peraluminous granites. In addition, CIPW calculations revealed that pegmatites and leucogranites contain at least 1.8 wt% normative corundum, thus indicating that they belong to the S-type category. Furthermore, the Na_2O content of the Sivigia pegmatite is 2.22 wt%, i.e., considerably lower than the maximum value of 3.2 wt% observed for S-type granites with a K_2O content of approximately 5 wt.% (CHAPPELL and WHITE, 1974). The Al#, the presence of 1.84 wt% normative corundum, and the Na_2O content thus suggest that the Sivigia pegmatite represents an S-type granite, in agreement with the high $\delta^{18}O_{SMOW}$ values. However, the same cannot be said for the Val Bona pegmatite, because its Na_2O content of 3.63 wt% points to an I-type granite, even though its Al# and its CIPW normative corundum value suggest an S-type origin.

The garnet-bearing Novate granite is distinct from both Sivigia and Val Bona pegmatites: its total alkali content and Al# are lower, its Na_2O content is greater than 3.2 wt%, and its CIPW norma-

Tab. 9 Rare Earth Element composition (in ppm) of the studied pegmatites and other igneous rocks from the Bergell area.

	Sivigia Pegmatite	Val Bona Pegmatite	Pegmatite	Novate Granite	Leucogranite	Bergell Tonalite	Bergell Granodiorite
Sample #	BV1	Peg1	Siss7	PS-8	C87-9	PS-2, -3, -5 (Mean)	PS-11, -12, -13 (Mean)
Swiss Coordinates	763.500/ 129.140	776.300/ 132.840	777.350/ 131.500	755.500/ 121.300	764.075/ 129.700	various	various
La	2.55	3.4	4.5	12.8	13.8	26.1	48.2
Ce	7	7	8.6	23.4	26.5	56.1	88.7
Pr	0.9	0.8	n.a.	n.a.	n.a.	n.a.	n.a.
Nd	3.35	3.6	6.383	11.6	11.3	29.2	35.6
Sm	1.75	1.05	1.848	2.38	2.91	5.93	5.67
Eu	0.05	0.17	0.2	0.50	0.64	1.35	1.08
Gd	1.55	0.95	n.a.	n.a.	n.a.	n.a.	n.a.
Tb	0.35	0.25	0.3	0.28	0.44	0.80	0.51
Dy	2.6	1.35	n.a.	n.a.	n.a.	n.a.	n.a.
Ho	0.365	0.26	n.a.	n.a.	n.a.	n.a.	n.a.
Er	1.2	0.65	n.a.	n.a.	n.a.	n.a.	n.a.
Tm	0.2	0.15	n.a.	n.a.	n.a.	n.a.	n.a.
Yb	2.15	1	1.7	0.90	0.92	2.58	1.33
Lu	0.26	0.17	0.2	0.15	0.13	0.43	0.22

BV1 and Peg1 are our own samples analyzed by XRAL Laboratories using ICPMS. The detection limit was 0.2 ppm for Pr, 0.05 ppm for Eu, Ho and Lu, and 0.1 ppm for all other elements. The data for Siss7 are from VON BLANCKEN-BURG et al. (1992), for C87-9 are from DIETHELM (1989). All other data are from MOTTANA et al. (1978). n.a. = not analyzed.

Tab. 10 Garnet-quartz ratios in the pegmatite samples from Bergell, Adamello and Gaya District, India.

Locality		Sample	Area Covered (cm²)	area %		wt %		mol %	
				Garnet	Quartz	Garnet	Quartz	Garnet	Quartz
Sivigia	BV4b	Fe & Si maps	ca. 0.9	46.6	53.4	58.2	41.8	14.4	85.6
		Mn & Si maps	ca. 0.9	46.8	53.2	58.4	41.6	14.5	85.5
		Al & Si maps	ca. 0.9	47.2	52.8	58.8	41.2	14.7	85.3
		Mean X-ray maps	ca. 0.9	46.9	53.1	58.5	41.5	14.6 (± 0.2)	85.4 (± 0.2)
	BV4a	Thin section (scanned)	ca. 1.2	59.8	40.2	70.3	29.7	22.3	77.7
	BV4b	Thin section (scanned)	ca. 1.8	56.8	43.2	67.8	32.2	20.3	79.7
	BV4b	4 photomicrographs (scanned)	ca. 2.8	52.5	47.5	63.8	36.2	17.6	82.4
	BV4	Photo of hand specimen	ca. 12.9	43.2	56.8	54.8	45.2	12.8	87.2
	Mean Sivigia			**50.4**	**49.6**	**61.7**	**38.3**	**16.7 (± 3.5)**	**83.3 (± 3.5)**
Val Bona	Specimen 1	Photo 1	ca. 1.8	69.3	30.7	78.3	21.7	30.4	69.6
		Photo 2	ca. 1.9	70.1	29.9	79.0	21.0	31.3	68.7
		Slide 2-1	ca. 1.7	68.5	31.5	77.6	22.4	29.6	70.4
		Slide 2-2	ca. 2.0	69.3	30.7	78.3	21.7	30.4	69.6
		Mean Specimen 1		69.3	30.7	78.3	21.7	30.4 (± 0.7)	69.6 (± 0.7)
	Specimen 2	Area 1		63.0	37.0	73.1	26.9	24.8	75.2
		Area 2		52.6	47.4	64.0	36.0	17.7	82.3
		Mean Specimen 2		57.8	42.2	68.5	31.5	21.2	78.8
	Mean Val Bona			**65.5**	**34.5**	**75.1**	**24.9**	**27.4 (± 5.3)**	**72.6 (± 5.3)**
Adamello	AU18A	Photomicrographs (Parts 1 and 2)	ca. 1.3	55.3	44.7	66.3	33.7	19.3	80.7
	269a	Thin section (scanned)	ca. 2.1	41.8	58.2	53.4	46.6	12.2	87.8
	Mean Adamello			**48.6**	**51.4**	**59.8**	**40.2**	**15.7**	**84.3**
Gaya District, India		Roy (1935)	–	–	–	73.0	27.0	25.0	75.0

The Si, Fe, Mn and Al X-ray maps for sample BV4b were processed by NIH Image (1.61/fat) to obtain the garnet: quartz ratios. All others were processed by MultiSpec (Version 3.8), developed by the Laboratory for Applications of Remote Sensing at Purdue University.

Standard deviations given for the means (in brackets) are listed as $1\sigma_{n-1}$.

In the following, D_m = measured density (in g/cm³), W_F = formula weight (in g/mol). The D_m and D_c values of Almandine, Spessartine, and Quartz are from NICKEL and NICHOLS (1991): *Almandine:* D_m = 4.318, D_c = 4.29, W_F = 497.75338; *Spessartine:* D_m = 4.18, D_c = 4.21, W_F = 495.02638; *α-Quartz:* D_m = 2.655, D_c = 2.651, W_F = 60.0843.

D_m(calc) and W_F(calc) were calculated as follows using weight proportions of the constituting end-members for each locality:

- BV4a, BV4b, and BV4 are from the same locality (Sivigia, Bergell) where Almandine ≈ 40 mol % and Spessartine ≈ 60 mol%.
  D_m(calc) = 4.2352, W_F(calc) = 496.11718.
- Sample from Val Bona (Bergell): Almandine ≈ 50 mol %, Spessartine ≈ 50 mol %. D_m(calc) = 4.249, W_F(calc) = 496.38988.
- AU18A is from Val Caffaro, Adamello: Almandine≈ 30 mol%, Spessartine ≈ 70 mol%. D_m(calc) = 4.2214, W_F(calc) = 495.84448.

For the sample from India, we assumed that garnet was composed of 50 mol% Almandine and 50 mol% Spessartine.

tive corundum value is only 1.12 wt%. These data thus document that the Novate granite represents a transition between I- and S-type. Isotopic data further indicate that the Novate granite formed from a predominantly crustal source and that it is unrelated to the Bergell intrusion (VON BLANCK-ENBURG et al., 1992).

The occurrence of considerable amounts of spessartine-rich garnet might point to a significant concentration of manganese in the melt. Substantial bulk-rock MnO contents, however, were only found for the Sivigia pegmatite (0.34 wt%) and for a garnet-bearing muscovite pegmatite studied by WENGER and ARMBRUSTER (1991, sample MP-1, Tab. 8). The MnO content of the Val Bona pegmatite is low (0.01 wt%) and comparable to all other granitoid rocks from Bergell.

For the pegmatite samples from Sivigia and Val Bona, the rare earth element (REE) composition has additionally been determined (Tab. 9). Also listed in table 9 are literature data for some other igneous rocks of the Bergell pluton and for the Novate granite. The chondrite-normalized

REE patterns of the two pegmatites are relatively flat, and exhibit a negative Eu anomaly, which is particularly pronounced for the Sivigia sample (Fig. 9). Very similar REE patterns are also displayed by a muscovite pegmatite (sample Siss7) and an aplite from eastern Bergell (VON BLANCK-ENBURG et al., 1992). These patterns document that the dikes are depleted in REE relative to the older igneous rocks in the Bergell area. The negative Eu anomaly is probably caused by the selective incorporation of Eu^{2+} into anorthite-rich plagioclase during earlier stages of magma evolution, and with the removal of anorthite, the resulting magma is consequently depleted in Eu. The other rocks from Bergell do not exhibit marked Eu anomalies. The REE patterns of Novate granite and Bergell leucogranite are very similar to each other: both are LREE-enriched and lack a pronounced Eu anomaly, and thus are distinctly different from the pegmatites (Fig. 9). The Bergell tonalite and granodiorite are richer in REE, and their chondrite-normalized patterns are LREE-enriched, whereby the enrichment is strongest for
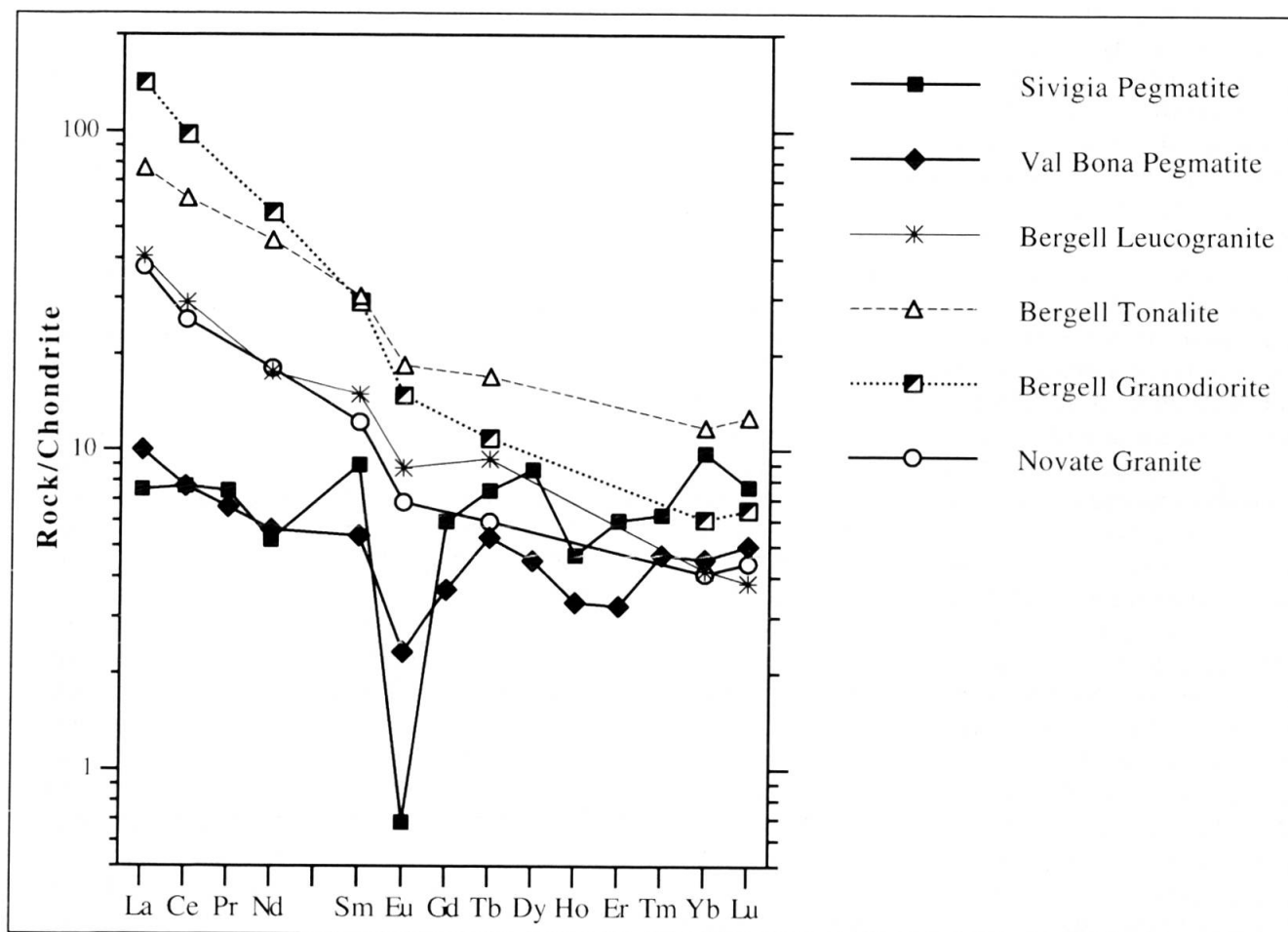

Fig. 9 Chondrite-normalized REE pattern of the Sivigia and Val Bona pegmatites, and other igneous rocks from the Bergell area. Chondrite values are from WAKITA et al. (1971). Data from table 9.

the granodiorite (see also VON BLANCKENBURG et al. 1992).

In summary, both the REE patterns and the major element characteristics document that the Sivigia and Val Bona pegmatites are distinct from the other garnet-bearing intrusive rocks in the Bergell area, i.e. Novate granite and leucogranites.

8. Discussion

8.1. ORIGIN OF GARNET

As outlined in the introduction, the presence of garnet in granitic rocks may be interpreted in various ways. At the studied localities, garnet is present in the country rocks and may also have been present in the source rocks of the pegmatite melts. Therefore, the possibility needs to be examined whether or not the garnets occurring in the intergrowths within the pegmatites might represent either remnant restite minerals or xenocrysts, which were later metasomatized by a Si-rich fluid. There are several arguments against such an interpretation: (1) the texture goniometry indicates the intergrowth of two single crystals of quartz and garnet for the Sivigia example. Such an intergrowth suggests that both minerals have crystallized simultaneously and is inconsistent with a later alteration or modification of an existing xenocryst or restite mineral; (2) at Sivigia, the statistically identical $\delta^{18}O$ values of quartz within and outside the garnet-quartz intergrowth (Tab. 6) provide evidence that both the nodule and the pegmatite matrix were formed during the same process, i.e., magmatic crystallization; (3) the oxygen isotope data, although only available for the Sivigia pegmatite, do not reveal significant postmagmatic hydrothermal alteration, consistent with the absence of extensive feldspar alteration; (4) the composition of garnet occurring in the country rocks of the Bergell pluton is distinctly different from that of the garnet in the intergrowths (GIERÉ, 1985; PERETTI, 1985; RUZICKA, 1997); (5) the quartz lamellae occurring within the intergrowths typically do not extend beyond the sharp (Fig. 4a) nodule boundaries into the pegmatite matrix (Figs 3a, 4b). On the other hand, where quartz lamellae do cross the nodule boundary, they become part of regular (graphic) intergrowths with alkali feldspar or muscovite in the pegmatite matrix (Figs 3d, 4c). This latter observation suggests that quartz grew simultaneously with garnet, and also with alkali feldspar and muscovite in the matrix, thus supporting the interpretation of garnet as product of magmatic crystalli-

zation. In summary, the observations and data suggest that the described graphic intergrowths are an igneous feature, formed through simultaneous crystallization of garnet and quartz from a pegmatite melt.

8.2. FORMATION OF GARNET-QUARTZ INTERGROWTHS

It has been suggested that comparable garnet-quartz intergrowths in a pegmatite dike near Gujandi, Gaya District, India were formed by eutectic crystallization (ROY, 1935). Although our data strongly indicate a magmatic origin, eutectic crystallization probably does not adequately describe the formation of the studied intergrowths. This is inferred particularly from the compositional zoning observed in many of the garnet lamellae. While garnet is homogeneous in the Val Bona intergrowth, more than half of all analyzed garnet lamellae at Sivigia and Adamello exhibit normal zoning. Compositional zoning was further reported by SUZUKI and MATSUMOTO (1989) for garnet occurring in similar garnet-quartz intergrowths from microcline pegmatite dikes on Nesöya Island, East Antarctica. At this locality, garnet is mainly an almandine-grossular solid solution (core: $Gros_{16.1}Alm_{71.2}Pyr_{5.5}Spes_{7.2}$, rim: $Gros_{14.1}Alm_{72.4}Pyr_{6.0}Spes_{7.2}$), in striking contrast to the spessartine- and almandine-rich compositions observed at the three localities studied here and also at the Oberpfalz locality in Germany (KECK, 1963). These data clearly demonstrate that the composition of garnet may vary considerably within individual intergrowths. This result is not consistent with eutectic crystallization, but rather points to cotectic crystallization. Additionally, the garnet composition is distinct at each locality, indicating that simultaneous crystallization of garnet and quartz may take place at different P-T conditions and in different melt compositions.

For the samples from India, ROY (1935)[2] reported a garnet-quartz ratio of approximately 73:27. For the intergrowths at Bergell and Adamello, the garnet-quartz ratios were initially determined as area ratios (see Tab. 10). If these are taken to be equivalent to volume ratios, and if it is further assumed that the density of garnet can be calculated from the densities of the constituting end-members simply by using the respective weight proportions, then the volume ratios can be converted to weight ratios, and finally to molar ratios. The aver-

---

[2] The author did not specify the kind of ratio, but judging from the context, it is probably a weight ratio.

age garnet-quartz molar ratios so obtained are approximately 17:83 for Sivigia, 27:73 for Val Bona, and 16:84 for Adamello (Tab. 10). Inspection of table 10 further reveals that these average ratios are associated with rather large standard deviations. At Sivigia, for example, the molar garnet-quartz ratio varies from 13:87 to 22:78. The reason for this variation is, at least in part, due to the fact that various types of input data were used: two different thin sections (BV4a and BV4b), one hand specimen photo (BV4), and three different combinations of X-ray maps. The areas covered by these different images are not the same, but vary from 0.9 cm^2 (X-ray maps) to 12.9 cm^2 (hand specimen, see Tab. 10). Moreover, the observed variation in garnet-quartz ratios might reflect a difference in the three-dimensional distribution of the two minerals. For the sample from India (ROY, 1935), the molar ratio of garnet to quartz is approximately 25:75, assuming that garnet is composed of equal amounts of spessartine and almandine. These results thus demonstrate that the average molar ratio of garnet to quartz can vary considerably in such intergrowths, ranging from about 1:3 (Val Bona and Gaya District) to 1:5 (Sivigia). This variation probably reflects the different conditions under which the intergrowths were formed.

8.3. CONDITIONS OF GARNET CRYSTALLIZATION

GREEN (1977, 1992) demonstrated that MnO had a considerable effect in stabilizing garnet in silicic liquids at relatively low pressures. He has shown that garnet with 20–25 mol% spessartine can form by equilibrium crystallization from a granitic melt at depths as shallow as 12 km, and that, with higher spessartine content, it may crystallize even at shallower levels. In all the studied intergrowths, garnet is substantially richer in spessartine component, i.e. approximately 50 mol% at the Val Bona locality, 54–64 mol% at Sivigia, and 61–78 mol% at Adamello. These high spessartine contents thus would be compatible with garnet crystallization at depths of less than 12 km, corresponding to pressures of less than approximately 4 kbar. Such a low pressure prevailed at the time of emplacement of the southern Adamello batholith, for which a confining total pressure of 2–3 kbar was estimated (RIKLIN, 1985; and unpublished Al-in-hornblende data from L. Matile, personal communication). The crystallization pressures at the time of emplacement of the main igneous mass of the Bergell pluton were determined to be higher than at Adamello. For the area

near the Sivigia pegmatite (floor of the pluton), the pressure was estimated at 6.4 ± 0.5 kbar (DAVIDSON et al., 1996), and for the Val Bona area (roof of the pluton), pressure estimates range from 3 kbar (PUSCHNIG, 1998) to approximately 5 kbar (REUSSER, 1999). The pressure estimates for Bergell have been obtained for the tonalite by using the Al-in-hornblende geobarometer, and thus may not be representative of the confining pressure at the time of the pegmatite emplacement. Field observations clearly show that the pegmatites in the Bergell area are younger than both tonalite and granodiorite, i.e. younger than 30 Ma (VON BLANCKENBURG, 1992). The relationship between the Novate granite and the studied Bergell pegmatites, however, is unknown, since no direct cross-cutting relationships were observed in the field. The pegmatites may thus be even younger than the Novate granite dated at 25 Ma (KÖPPEL and GRÜNENFELDER, 1975; HANSMANN, 1996). At this time, the confining pressures probably have been considerably less than those estimated for the tonalite crystallization, because the Bergell area underwent a rapid exhumation until shortly after the intrusion of the Novate granite (for review, see HANSMANN, 1996). The pressures at the time of pegmatite emplacement in the Bergell area, thus, are possibly comparable to those estimated for the southern Adamello. The high spessartine contents of the Sivigia and Val Bona garnets are compatible with this conclusion.

9. Conclusions

From the data presented here, we conclude that the graphic intergrowths of garnet and quartz described for the three pegmatite localities are the result of simultaneous crystallization of garnet and quartz from a granitic melt. The high spessartine content of garnet in these intergrowths suggests that simultaneous crystallization of garnet and quartz in granitic melts is possible at shallow crustal levels. We further conclude from our observations and data that the graphic intergrowths of garnet and quartz are the result of cotectic rather than eutectic crystallization.

provided excellent reviews that significantly improved this paper. Additionally, we wish to thank the late Dr. Martin Frey (Basel) for his help as an editor of this manuscript. We thank the authors of the software packages NIH Image (1.61/fat) and MultiSpec (Version 3.8), which were used for processing of images and photos.

References

ABBOTT, R.N., Jr. (1981): AFM liquidus projections for granitic magmas, with special reference to hornblende, biotite and garnet. Can. Mineral. 19, 103–110.

ABBOTT, R.N., Jr. and CLARKE, D.B. (1979): Hypothetical liquidus relationships in the subsystem Al_2O_3–FeO–MgO projected from quartz, alkali feldspar and plagioclase for $a(H_2O) <$ or $= 1$. Can. Mineral. 17, 549–560.

ALLAN, B.D. and CLARKE, D.B. (1981): Occurrence and origin of garnets in the South Mountain Batholith, Nova Scotia. Can. Mineral. 19, 19–24.

BALDWIN, J.R. and VON KNORRING, O. (1983): Compositional range of Mn-garnet in zoned granitic pegmatites. Can. Mineral. 21, 683–688.

BELLIENI, G., MOLIN, G.M. and VISONA, D. (1979): The petrogenetic significance of the garnets in the intrusive massifs of Bressanone and Vedrette di Ries (Eastern Alps–Italy). N. Jb. Mineral. (Abh.) 136, 238–253.

BERGER, A., ROSENBERG, C. and SCHMID, S.M. (1996): Ascent, emplacement and exhumation of the Bergell pluton within the Southern Steep Belt of the Central Alps. Schweiz. Mineral. Petrogr. Mitt. 76, 357–382.

BIANCHI, A., CALLEGARI, E. and JOBSTRAIBIZER, P.G. (1970): I tipi petrografici fondamentali del plutone dell'Adamello: tonaliti, quarzodioriti, granodioriti e loro varieta leucocrate. Memorie degli Istituti di Geologia e Mineralogia dell' Universita di Padova 27, 1–146.

BIRCH, W.D. and GLEADOW, A.J.W. (1974): The genesis of garnet and cordierite in acid volcanic rocks: evidence from the Cerberean Cauldron, Central Victoria, Australia. Contrib. Mineral. Petrol. 45, 1–13.

BLUNDY, J.D. and SPARKS, R.S.J. (1992): Petrogenesis of mafic inclusions in granitoids of the Adamello Massif, Italy. J. Petrol. 33, 1039–1104.

BOGOCH, R., BOURNE, J., SHIRAV, M. and HARNOIS, L. (1997): Petrochemistry of a Late Precambrian garnetiferous granite, pegmatite and aplite, southern Israel. Mineral. Mag. 61, 111–122.

BOTTINGA, Y. and JAVOY, M. (1973): Comments on oxygen isotope geothermometry. Earth Planet. Sci. Lett. 20, 250–265.

BOTTINGA, Y. and JAVOY, M. (1975): Oxygen isotope partitioning among the minerals in igneous and metamorphic rocks. Reviews of Geophysics and Space Physics 13, 401–418.

BRACK, P. (1984): Geologie der Intrusiva und Rahmengesteine des Südwest-Adamello (Nord-Italien). Ph.D. Thesis. Nr. 7612, ETH Zürich, 253 pp.

BRACK, P. (1985): Multiple intrusions – examples from the Adamello Batholith (Italy) and their significance on the mechanisms of intrusion. Mem. Soc. Geol. It. 26, 145–157.

BROUSSE, R. and MAURY, R. (1976): Paragenese manganesifere d'une rhyolite hyperalcaline du Mont–Dore. Bulletin de la societé francaise de minéralogie et de cristallographie 99, 300–303.

CALLEGARI, E. (1966): I granati di alcuni differenziazioni aplitico-pegmatitiche del Massiccio dell'Adamello. Memorie della Accademia Patavina Sc. Lett. A., Cl. Sc. Mat. Nat. 78, 363–377.

CALLEGARI, E. (1985): Geological and petrological aspects of the magmatic activity at Adamello (Northern Italy). Mem. Soc. Geol. It. 26, 83–103.

CALLEGARI, E. and DAL PIAZ, G.B. (1973): Field relationships between the main igneous masses of the Adamello Intrusive massif (Northern Italy). Memorie dell' Istituto di Geologia e Mineralogia, Università di Padova 31, 1–34.

CHAPPELL, B.W. and WHITE, A.J.R. (1974): Two contrasting granite types. Pacific Geology 8 (Circum–Pacific plutonism), 173–174.

CLARKE, D. B. (1981): The mineralogy of peraluminous granites: a review. Can. Mineral. 19, 3–17.

CLARKE, D.B. and ROTTURA, A. (1994): Garnet-forming and garnet-eliminating reactions in a quartz diorite intrusion at Capo Vaticano, Calabria, Southern Italy. Can. Mineral. 32, 623–635.

CLAYTON, R.N. and MAYEDA, T.K. (1963): The use of bromine pentafluoride in the extraction of oxygen from oxides and silicates for isotopic analysis. Geochim. Cosmochim. Acta 27, 43–52.

DANA, J.D., DANA, E.S. and GAINES, R.V., (1997): Dana's New Mineralogy: The system of mineralogy of James Dwight Dana and Edward Salisbury Dana. Wiley, New York, 1819 pp.

DAVIDSON, C., ROSENBERG, C. and SCHMID, S.M. (1996): Synmagmatic folding of the base of the Bergell pluton, Central Alps. Tectonophysics 265, 213–238.

DEL MORO, A., PARDINI, G., QUERCIOLI, C., VILLA, I.M. and CALLEGARI, C. (1983): Rb/Sr and K/Ar chronology of Adamello granitoids, southern Alps. Mem. Soc. Geol. It. 26(1), 285–299.

DIETHELM, K. (1989): Petrographische und geochemische Untersuchungen an basischen Gesteinen der Bergeller Intrusion. Ph.D. Thesis. Nr. 8855, ETH Zürich, 152 pp.

DRAKE, M.J. and WEILL, D.F. (1972): New rare earth element standards for electron microprobe analysis. Chem. Geol. 10, 179–181.

DU BRAY, E.A. (1988): Garnet compositions and their use as indicators of peraluminous granitoid petrogenesis; southeastern Arabian Shield. Contrib. Mineral. Petrol. 100, 205–212.

EPSTEIN, S. and TAYLOR, H.P., Jr. (1967): Variation of O^{18}/O^{16} in minerals and rocks. In: ABELSON, P. H. (ed.): Researches in Geochemistry 2, 29–62. John Wiley, New York.

FOORD, E.E. (1976): Mineralogy and Petrogenesis of Layered Pegmatite Aplite Dikes in the Mesa Grande District, San Diego County, California. Ph.D. Thesis, Stanford Univ., USA.

GIERÉ, R. (1984): Geologie und Petrographie des Bergell-Ostrandes. M.S. Thesis, ETH Zürich, Switzerland, 175 pp.

GIERÉ, R. (1985): Metasedimente der Suretta-Decke am Ost- und Südostrand der Bergeller Intrusion: Lithostratigraphische Korrelation und Metamorphose. Schweiz. Mineral. Petrogr. Mitt. 65, 57–78.

GIERÉ, R. (1987): La geologia tra le valli Sissone e Muretto. Val Malenco. Natura 1. Atti ufficiali del convegno (in Italian), 21–26.

GREEN, T.H. (1977): Garnet in Silicic Liquids and Its Possible Use as a P-T Indicator. Contrib. Mineral. Petrol. 65, 59–67.

GREEN, T.H. (1992): Experimental phase equilibrium studies of garnet-bearing I-type volcanics and high-level intrusives from Northland, New Zealand.

Transactions Royal Soc. Edinburgh, Earth Sci. 83, 429–438.

HAFNER, M. (1993): Strukturgeologische und geochemische Untersuchungen von leukokraten Granitgängen und Migmatiten der südlichen Adula am Monte Peschiera (It). M.S. Thesis, Univ. Basel, Switzerland, 82 pp.

HALL, A. (1965): The origin of accessory garnet in the Donegal Granite. Mineralogical Magazine and Journal of the Mineralogical Society 35, 628–633.

HANSMANN, W. (1996): Age Determinations on the Tertiary Masino–Bregaglia (Bergell) Intrusives (Italy, Switzerland): a review. Schweiz. Mineral. Petrogr. Mitt. 76, 421–451.

HARRISON, T.N. (1988): Magmatic garnets in the Cairngorm Granite, Scotland. Mineral. Mag. 52, 659–667.

HENTSCHKE, U. (1987): The genetic significance of garnets in the plutonic complexes of the Harz Mountains. N. Jb. Mineral. (Abh.) 156, 141–153.

HSU, L.C. (1968): Selected Phase Relationships in the System Al–Mn–Fe–Si–O–H: A Model for Garnet Equilibria. J. Petrol. 9, 40–83.

JAFFE, H.W. (1951): The Role of Yttrium and Other Minor Elements in the Garnet Group. Am. Mineral. 36, 133–155.

JAMIESON, R.A. (1974): The contact of the South Mountain Batholith near Mt. Uniacke, Nova Scotia. B.S. Thesis, Dalhousie University, Halifax, Nova Scotia, Canada.

JOYCE, A.S. (1973): Chemistry of the minerals of the granitic Murrumbidgee Batholith, Australian Capital Territory. Chem. Geol. 11, 271–296.

KAGAMI, H., ULMER, P., HANSMANN, W., DIETRICH, V. and STEIGER, R.H. (1991): Nd-Sr isotopic and geochemical characteristics of the southern Adamello (Northern Italy) intrusives: Implications for crustal versus mantle origin. J. Geophys. Res. 96, 14331-14346.

KASOWSKI, M.A. and HOGARTH, D.D. (1968): Yttrian andradite from the Gatineau Park, Quebec. Can. Mineral. 9, 552–558.

KECK, E. (1963): Oberpfälzer Granate – Vorkommen und chemische Zusammensetzung. Der Aufschluss 14, 316-320.

KÖPPEL, V. and GRÜNENFELDER, M. (1975): Concordant U-Pb ages of monazite and xenotime from the Central Alps and the timing of the high temperature Alpine metamorphism; a preliminary report. Schweiz. Mineral. Petrogr. Mitt. 55, 129-132.

KROT, A.N., RUBIN, A.E. and KONONKOVA, N.N. (1993): First occurrence of Pyrophanite (Mntio$_3$) and Baddeleyite (ZrO$_2$) in an ordinary Chondrite. Meteoritics 28, 232–239.

LEAKE, B.E. (1967): Zoned garnets from the Galway granite and its aplites. Earth Planet. Sci. Lett. 3, 311–316.

LIIPO, J.P., VUOLLO, J.I., NYKANEN, V.M. and PIIRAINEN, T.A. (1994): Pyrophanite and ilmenite in serpentinized wehrlite from Ensila, Kuhmo Greenstone Belt, Finland. Eur. J. Mineral.6, 145–149.

LINHARDT, E. (2000): Der Beryllpegmatit der Feldspatgrube Maier, Püllersreuth. Lapis 3/2000, 13-23.

LONDON, D. (1996): Granitic pegmatites. Transactions of the Royal Society of Edinburgh: Earth Sciences 87, 305–319.

MACLEOD, G. (1992): Zoned manganiferous garnets of magmatic origin from the Southern Uplands of Scotland. Mineral. Mag. 56, 115–116.

MANNING, D.A.C. (1983): Chemical variation in garnets from aplites and pegmatites, peninsular Thailand. Mineral. Mag. 47, 353–358.

MATTHEWS, A., GOLDSMITH, J.R. and CLAYTON, R.N. (1983): Oxygen isotope fractionation between zoisite and water. Geochim. Cosmochim. Acta 47, 645–654.

MCCOY, T.J., EHLMANN, A.J. and MOORE, C.B. (1997): The Leedey, Oklahoma, chrondrite; fall, petrology, chemistry and an unusual Fe, Ni–FeS inclusion. Meteoritics and Planetary Science 32, 19–24.

MILLER, C.F. and STODDARD, E.F. (1978): Origin of garnet in granitic rocks; an example of the role of Mn from the Old Woman – Piute Range, California. Abstracts with Programs – Geological Society of America 10, 456.

MILLER, C.F. and STODDARD, E.F. (1981): The role of Manganese in the paragenesis of magmatic garnet: an example from the Old Woman – Piute Range, California. J. Geol. 89, 233–246.

MOTICSKA, V.P. (1970): Petrographie und Strukturanalyse des westlichen Bergeller Massivs und seines Rahmens. Schweiz. Mineral. Petrogr. Mitt. 50, 355–443.

MOTTANA, A., MORTEN, L. and BRUNFELT, A.O. (1978): Distribuzione Delle Terre Rare Nel Massiccio Val Masino–Val Bergaglia (Alpi Centrali). Rend. Soc. Ital. Mineral. Petrol. 34, 485–497.

MÜCKE, A. and WOAKES, M. (1986): Pyrophanite: a typical mineral in the Pan-African Province of Western and Central Nigeria. Journal of African Earth Sciences 5, 675–689.

NICKEL, E.H. and NICHOLS, M.C. (eds)(1991): Mineral reference manual. Van Nostrand Reinhold, New York.

PERETTI, A. (1985): Der Monte–del–Forno–Komplex am Bergell-Ostrand: Seine Lithostratigraphie, alpine Tektonik und Metamorphose. Eclogae geol. Helv. 78, 23–48.

PORTNOV, A.M. (1963): Pyrophanite from northern Baikalia. Doklady of the Academy of Sciences of the U.S.S.R. Earth sciences sections 153, 126–128.

PUSCHNIG, A.R. (1998): The Forno unit (Rhetic Alps): Evolution of an ocean floor sequence from rifting to Alpine orogeny. Ph.D. Thesis. Nr. 12702, ETH Zürich, 204 pp.

PUZIEWICZ, J. (1990): Post-magmatic origin of almandine–spessartine garnet in the Strzeblow alaskite (Strzegom–Sobotka granitic massif, SW–Poland). N. Jb. Mineral. (Mh.) 1990, 168–175.

REUSSER, C. E. (1987): Phasenbeziehungen im Tonalit der Bergeller Intrusion. Ph.D. Thesis. Nr. 8329, ETH Zürich, 220 pp.

REUSSER, E. (1999): Epidote of magmatic origin in the tonalite of the Bergell Pluton, Central Alps. European Union Of Geosciences, Strasbourg, France, Journal Of Conference Abstracts 4, 721.

RIKLIN, K. (1985): Contact Metamorphism of the Permian „Red Sandstone" in the Adamello area. Mem. Soc. Geol. It. 26, 159–169.

ROSENBAUM, J. M. and MATTEY, D. (1995): Equilibrium garnet–calcite oxygen isotope fractionation. Geochim. Cosmochim. Acta 59, 2839–2842.

ROY, A.K. (1935): A garnet–quartz intergrowth with the outer form of garnet. Proceedings of the Indian Science Congress, 211.

RUZICKA, R.J.W. (1997): Der Nordrand des Gruf–Komplexes und seine Beziehung zur Engadiner Linie. M.S. Thesis, Univ. Basel, Switzerland, 81 pp.

SATHE, R.V. (1968): Grossular–spessartine garnet from Goldongri, Panchmahal, Gujarat state, India. Mineral. Mag. 36, 1032–1033.

SCHMID, S.M., BERGER, A., DAVIDSON, C., GIERÉ, R., HERMANN, J., NIEVERGELT, P., PUSCHNIG, A.R. and ROSENBERG, C. (1996): The Bergell pluton (South-

ern Switzerland, Northern Italy): overview accompanying a geological–tectonic map of the intrusion and surrounding country rocks. Schweiz. Mineral. Petrogr. Mitt. 76, 329–355.

SMITH, J.V. (1974): Feldspar minerals 2: Chemical and Textural Properties. Ed. Springer-Verlag, Berlin, New York. 690 pp.

SOKOLOV, Y.M. and KHLESTOV, V.V. (1990): Garnets as indicators of the physicochemical conditions of pegmatite formation. International Geology Review 32, 1095–1107.

STONE, M. (1988): The significance of almandine garnets in the Lundy and Dartmoor granites. Mineral. Mag. 52, 651–658.

SUZUKI, M. and MATSUMOTO, Y. (1989): Pegmatite from Nesöya Island, Lützowholm bay, East Antarctica: with special reference to garnet-quartz symplektite (Abstract). Proceedings of the NIPR Symposium on Antarctic Geosciences 3, 151.

TAYLOR, H.P., Jr. and EPSTEIN, S. (1962): Relationship between O^{18}/O^{16} ratios in coexisting minerals of igneous and metamorphic rocks. Part 1: Principles and experimental results. Geol. Soc. Am. Bull. 73, 461–480.

TOMKEIEFF, S.I. (1983): Dictionary of petrology. Edited by: WALTON, E.K., RANDALL, B.A.O., BATTEY, M.H. and TOMKEIEFF, O. Wiley, Chichester, New York, 680 pp.

TROMMSDORFF, V. and NIEVERGELT, P. (1985): The Bregaglia (Bergell) Iorio intrusive and its field relations. Mem. Soc. Geol. It. 26, 55–68.

ULMER, P. (1982): Geologie und Petrographie des südlichen Adamello: VIII. Valle del Caffaro. M.S. Thesis, ETH Zürich, 134 pp.

ULMER, P., CALLEGARI, E. and SONDEREGGER, U.C. (1985): Genesis of the mafic and ultramafic rocks and their genetical relations to the tonalitic–trondhjemitic granitoids of the southern part of the Adamello Batholith, (Northern Italy). Mem. Soc. Geol. It. 26, 171–222.

VENNUM, W.R. and MEYER, C.E. (1979): Plutonic garnets from the Werner batholith, Lassiter Coast, Antarctic Peninsula. Am. Mineral. 64, 268–273.

VON BLANCKENBURG, F. (1992): Combined high-precision chronometry and geochemical tracing using accessory minerals: applied to the Central-Alpine Bergell intrusion. Chem. Geol. 100, 19–40.

VON BLANCKENBURG, F., FRÜH-GREEN, G., DIETHELM, K. and STILLE, P. (1992): Nd-, Sr-, O-isotopic and chemical evidence for a two-stage contamination history of mantle magma in the Central-Alpine Bergell intrusion. Contrib. Mineral. Petrol. 110, 33–45.

WAKITA, H., REY, P. and SCHMITT, R.A. (1971): Abundances of the 14 rare-earth elements and 12 other trace elements in Apollo 12 samples; five igneous and one breccia rocks and four soils. Geochim. Cosmochim. Acta 2, 1319–1329.

WEIGAND, P.W., PARKER, J. and COLLINS, L.G. (1981): Metamorphic origin of garnets in the Lowe Granodiorite, San Gabriel Mtns., California. EOS Trans. Am. Geophys. Union 62, 1060.

WENGER, M. and ARMBRUSTER, T. (1991): Columbite (Fe, Mn)(Nb, Ta)$_2$O$_6$ in the pegmatites of the calc–alkaline Bergell intrusion (southeast Central Alps). Schweiz. Mineral. Petrogr. Mitt. 71, 349–369.

WENK, H.R. and CORNELIUS, S.B. (1977): Geologischer Atlas der Schweiz, Blatt 1296 (Sciora). Published by Schweiz. Geol. Komm.

WENK, H.R., HSIAO, J., FLOWERS, G., WEIBEL, W., AYRANCI, B. and FEJER, Z. (1977): A geochemical survey of granitic rocks in the Bergell Alps. Schweiz. Mineral. Petrogr. Mitt. 57, 233–265.

WHITE, A.J.R. and CHAPPELL, B.W. (1977): Ultrametamorphism and granitoid genesis. Tectonophysics 43, 7–22.

WHITWORTH, M.P. (1992): Petrogenetic implications of garnets associated with lithium pegmatites from SE Ireland. Mineral. Mag. 56, 75–83.

YERMOLOV, P.V., IZOKH, A.E. and VLADIMIROV, A.G. (1979): Garnet as an indicator of conditions of granite formation in the crust. Doklady Akademii Nauk SSSR 245, 208–211.

ZECK, H.P. (1970): An erupted migmatite from Cerro del Hoyazo, SE Spain. Contrib. Mineral. Petrol. 26, 225–246.

ZHENG, Y.-F. (1993a): Calculation of oxygen isotope fractionation in anhydrous silicate minerals. Geochim. Cosmochim. Acta 57, 1079–1091.

ZHENG, Y.-F. (1993b): Calculation of oxygen isotope fractionation in hydroxyl–bearing silicates. Earth Planet. Sci. Lett. 120, 247–263.

APPENDIX – ANALYTICAL TECHNIQUES

Electron microprobe analysis

All electron microprobe analyses and X-ray maps were performed with a CAMECA SX-50 equipped with 4 crystal spectrometers at the Department of Earth and Atmospheric Sciences, Purdue University. The minerals were analyzed quantitatively at 15 kV and 20 nA, with a beam diameter of approximately 1 μm (10 μm for micas). Standards used were synthetic and natural compounds: apatite for F; diopside-jadeite for Na, Mg, Al, Si, and Ca; orthoclase for K; ScPO$_4$ for Sc; Ti-bearing diopside for Ti in silicates, ilmenite for Ti and Fe in magnetite and ilmenite; olivine for Fe in silicates; hortonolite for Mn; Corning glass for Rb; benitoite for Ba; and one of the Rare Earth glasses of DRAKE and WEILL (1972) for Y. The counting time on the peak was 20–30 s for major elements, and at least 60 s for trace elements. Counting time

on the background positions on either side of the peak was generally half of that on the corresponding peak. Where appropriate, only one side of the background was counted and an experimentally determined slope was adopted to calculate the background on the other side.

X-ray mapping

The spatial distribution of Mn, Fe, Mg, and Ca was imaged by producing X-ray maps at 15 kV and 20 nA (wavelength-dispersive mode, stationary beam). The maps were collected over an area of 1024 × 1024 square pixels with a step size of 10 μm and a dwelling time of 20 ms per pixel.

X-ray texture goniometry

Two garnet-quartz nodules (one each from Bergell and Adamello) have been studied by X-ray texture goniometry using a Siemens D5000 automated texture goniometer at the Geologisch-Paläontologisches Institut, Universität Basel. The measuring conditions have been 45kV acceleration voltage at 30 mA using a Co radiation source. Samples were measured in reflection mode to 85-degree-tilt on polished sections. The quartz $(10\bar{1}1)$-, $(10\bar{1}0)$-, and garnet (400)-reflections were found to produce the least interference of reflections and yielded a good representation of the orientation of the two minerals.

Oxygen isotope analysis

Fresh pieces broken from sample BV4 from Sivigia (Bergell) were ground, sieved, washed with distilled water, and dried at 120 °C for 8 h. From the portion with a grain size between 1.0 and 2.0 mm, separates of garnet, quartz, and plagioclase were prepared by hand-picking under a binocular microscope. For the plagioclase separate, only those grains exhibiting polysynthetic twinning were selected. The muscovite separate was picked directly from the sample, whereby the large and thick muscovite sheets were stripped to thin sheets, and examined under a binocular microscope to ensure their purity. Oxygen gas was extracted from the mineral separates by reaction with BrF_5 at 570–600 °C in Ni reaction vessels according to the procedures of CLAYTON and MAYEDA (1963). Quartz, plagioclase, and muscovite separates were reacted without further grinding at 570 °C for 8 h to release oxygen. Because garnet

reacts less readily with BrF_5, it was ground into a fine powder and reacted with BrF_5 for 24 hours and at 600 °C. The reaction yields all exceeded 97‰. Mass spectrometric analyses were performed on CO_2 obtained by converting the oxygen gas by combustion with a resistance-heated graphite rod (TAYLOR and EPSTEIN, 1962). The mass spectrometer used is a 60-degree, single-focusing, double-collecting, dual gas-feed, Nier-McKinney instrument. The overall analytical error is estimated at 0.1–0.2‰. In the course of this study, a working standard (NBS-28, with an assigned $\delta^{18}O$ value of 9.6‰) was included in the set of six samples analyzed. Three additional samples obtained from the BV4 hand specimen (the same garnet separate as above, and two quartz separates from within and outside the garnet-quartz intergrowth) were analyzed by the XRAL Laboratories (Toronto, Canada), which applied the same oxygen extraction method, but used a laboratory quartz standard calibrated relative to NBS-28. The reaction yields of 97.6% and 100.1% for quartz within and outside the intergrowth, respectively, are very good.

Whole-rock analysis

Two pegmatite samples from Bergell, one each from Sivigia and Val Bona, were analyzed by X-ray fluorescence spectroscopy (XRF) for major and some trace elements, and by inductively coupled plasma mass spectrometry (ICPMS) for rare earth elements (REE). The ferrous iron content was determined by titration, and the ferric iron content was then calculated from the total iron. All analyses were performed by XRAL Laboratories (Toronto, Canada) on aliquots prepared from approximately 500 g of rock powder.

Image processing

Various types of images have been examined by image processing software to obtain the garnet-quartz ratios in the intergrowths. X-ray maps were processed with *NIH Image 1.61/fat* because these images are simple grayscale pictures with only two categories (garnet and quartz). For color photographs (scanned thin sections, hand specimen photos, and microscopic pictures), we used *MultiSpec 3.8* (developed by the Laboratory for Applications of Remote Sensing, Purdue University).